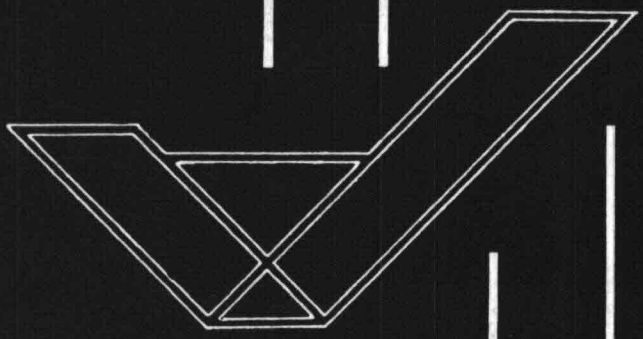

Reproduction of Velocity Profiles in Estuaries by some One-Dimensional Mathematical Models

R. Booij

Report no. 3-82

Laboratory of Fluid Mechanics
Department of Civil Engineering
Delft University of Technology

REPRODUCTION OF VELOCITY PROFILES IN ESTUARIES BY SOME ONE-DIMENSIONAL MATHEMATICAL MODELS

R. Booij

Report no. 3 - 82

Laboratory of Fluid Mechanics
Department of Civil Engineering
Delft University of Technology
Delft, The Netherlands

Summary

For the prediction of dispersion phenomena and of changes in the morphology of an alluvial bottom, a detailed description of the water flow is necessary. The flow in estuaries is a complicated one, partly because of the time-dependence. To isolate this aspect of tidal flow a simplifying one-dimensional (vertical) flow model is used. This one-dimensional model is obtained by the neglect of convective derivatives of the longitudinal velocity and the use of the rigid lid approximation, i.e. the replacement of the free surface by a flat frictionless plate. The error introduced by these approximations is not large for the flow in most tidal channels. Convective derivatives are generally of minor importance. The rigid lid approximation is inaccurate for tidal waves with a large ratio between wave height and water depth (e.g. > 1/10).

Tidal flow is usually described by simple eddy viscosity models in which various simple distributions of the eddy viscosity are prescribed. Recently models with an eddy viscosity depending on the turbulence energy, the k-model and the k-ε-model, have gained wide acceptance for all kinds of boundary layer flow. In this investigation the k-model and the k-ε-model are compared to an eddy viscosity model with an appropriate distribution of the eddy viscosity and to the mixing-length model for the case of steady and of time dependent free surface flow. The time dependent free surface flows,considered, represent flows in a tidal channel without a nett discharge over the tidal period. The roughness values and the velocities are typical for tidal channels.

The results of the various models differ hardly. The only appreciable difference is around slack water, where all models used are, however, less reliable. The close correspondence is explained by the short adjustment times of the turbulence energy and its dissipation compared to the tidal period and by the small relative roughness height. The flow in a tidal channel can be considered as slowly varying, showing almost logarithmic velocity profiles except around slack water. The hysteresis effect of the shear stress with respect to the surface velocity calculated with all these models is therefore small, in contradiction to the large hysteresis effect as found in some of the prototype measurements.

In all models some constants or the distribution of a length scale or an eddy viscosity have to be specified. In the k-ε-model only constants need to be specified. The physical bases of the k-model and certainly of the k-ε-model, however, are quite poor, throwing doubts on the constancy of the constants and the usefulness of the values of the constants beyond the direct situation of calibration. The k-ε-model is very sensitive to the values of most constants.

As the k-model and especially the k-ε-model require much smaller timesteps than a simple eddy viscosity model, the last model should be preferred whenever the specification of an eddy viscosity distribution is possible.

The conclusions arrived at, are generally valid for flows in tidal channels, as the considerations mentioned do not depend on the simplifications used.

This research was subsidized by the directorate of the Deltadienst of Rijkswaterstaat.

Contents

List of Figures

1. Introduction

For many problems in estuaries such as the transport and dispersion of pollutants, the behaviour of density differences and the changes in the morphology of the channel bed as a response to the influence of large hydraulic structures, a detailed knowledge of the water flow is indispensable. This knowledge is e.g. needed to calibrate depth-averaged models.

Until recently two kind of models accounting for vertical transport of momentum were in use, mixing length models and models using an eddy viscosity concept. Generally a simple vertical distribution of the eddy viscosity was chosen: a constant eddy viscosity; a combination of two different constant eddy viscosities,one for the near bed region and one for the remainder of the depth; etc. (see Knight, 1975).

In Booij (1981a) various models of this eddy viscosity type were compared. The comparison was executed in a one-dimensional vertical flow model, in which simple model the influence of tidal variation can be examined without topographical effects (See chapter 2). The best agreement with the measurements in tidal channels was obtained with an eddy viscosity that varied parabolic over depth and proportional to the depth-averaged velocity or the friction velocity. A good reproduction of the logarithmic velocity profiles as measured in most tidal phases and of the variation of velocity and shear stress with time were obtained. Only a hysteresis effect of the shear stress with respect to the surface velocity, that shows up in some measurements in tidal flow, did not reproduce.

Recently eddy viscosity models were developed that try to account for transport of turbulence and for the transport of its length scale. The models of this type, considered, are the k-model and the k-ε-model. The expectations of these models and especially of the k-ε-model for flows in rivers and estuaries are high (e.g. Rodi, 1980 and Delft Hydraulics Laboratory, 1973). An often cited investigation of the usability of those models for tidal channel flow was executed by Smith and Takhar (1979). Quite serious objections can however be raised against their treatment of the k-model and the k-ε-model. (see chapter 3 and 4).

In this investigation the mixing-length model, the k-model, the k-ε-model and the best simple eddy viscosity model are compared. This comparison is executed in the same one-dimensional flow model as used in Booij (1981a) for steady flow and flow in a tidal channel (chapter 4). The characteristic roughness height is given some typical values for tidal channels. Much attention is given to the constants and the length scale distribution to be specified in the various models (chapter 3). This also determines to which extent calibration of a model by variation of the constants as done by Smith and Takhar (1979) is allowed.

2 Mathematical Description

2.1 One-Dimensional Model of the Flow in a Tidal Channel

The model of the flow in a tidal channel used in this report is the one-dimensional model described in Booij (1981a).

A long-wave motion of small amplitude in a wide and straight open channel of constant width and depth is considered. In the absence of Coriolis accelerations and transverse oscillations, the motion is essentially two-dimensional. To describe this motion a rectangular coordinate system Ox, Oz is used, where Ox is situated on the bottom and directed along the channel and Oz is positive upwards (see fig. 1).

Following Proudman (1953) the shallow water equations are

$$\frac{\partial u}{\partial x} + \frac{\partial w}{\partial z} = 0 \tag{1}$$

$$\frac{\partial \zeta}{\partial t} + \frac{\partial}{\partial x} \int_0^{h+\zeta} u\,dz = 0 \tag{2}$$

$$\frac{Du}{Dt} = -s - \frac{\partial \tau}{\partial z} \tag{3}$$

In formula (3)

$$\frac{D}{Dt} = \frac{\partial}{\partial t} + u\frac{\partial}{\partial x} + w\frac{\partial}{\partial z} \tag{4}$$

is the Stokes derivative, u and w represent the ensemble-averaged velocities in the x and z direction respectively, τ is the horizontal kinematic Reynolds shear stress, h is the mean free surface level and $\zeta(x,t)$ its deplacement. The term s in equation (3) represents the kinematic pressure gradient, corresponding with the free surface slope

$$s = g\frac{\partial \zeta}{\partial x} \tag{5}$$

where g is the acceleration of gravity.

Replacing the Stokes derivative by the time derivative in equation (3) gives

$$\frac{\partial u}{\partial t} = -s - \frac{\partial \tau}{\partial z} \qquad (6)$$

The replacement of equation (3) by equation (6) corresponds to two approximations

- The rigid lid approximation. The free surface is represented by a flat frictionless plate. The pressure gradient corresponding with the free surface slope is maintained. This approximation is justified in the case of small vertical velocities and low waves.
- Convection of the velocity is neglected.

The error introduced by these approximations is not large in most flows in tidal channels (see Booij, 1981a). The rigid lid approximation is not justified in case of high tidal waves, causing large relative surface displacements, e.g. $|\zeta|/h>0.1$, and in case of bores. Convection of the velocity is generally of minor importance. The small flow velocities in the last few kilometers before a closed end of a tidal channel, however, lead to very small shear stresses. As a consequence convection can not be neglected there.

A one-dimensional model remains,if it is assumed that the Reynolds stress can be expressed in variables at the same x.

The model described above requires much less computational effort than the complete shallow water equations.

To solve equation (6),the shear stress τ has to be related to the other variables in this equation (the closure problem of turbulence.). Generally τ is related to the local mean velocity gradient by means of a (kinematic) eddy viscosity, $\nu_t(z,t)$, defined by

$$\tau = -\nu_t \frac{\partial u}{\partial z} \qquad (7)$$

Substitution in equation (6) yields

$$\frac{\partial u}{\partial t} - \frac{\partial}{\partial z}\left(\nu_t \frac{\partial u}{\partial z}\right) = -s \qquad (8)$$

Various turbulence models involving different relations between the eddy viscosity and other variables will be discussed in the next chapter.

Henceforth an imposed harmonic pressure gradient is considered

$$s = -S \cos \omega t \tag{9}$$

S is the amplitude of the varying pressure gradient. Equation (8) now reads

$$\frac{\partial u}{\partial t} - \frac{\partial}{\partial z} \left(\nu_t \frac{\partial u}{\partial z} \right) = S \cos \omega t \tag{10}$$

The resulting one-dimensional flow model is quite simple, but it allows the performances of the various turbulence models to be compared for a flow resembling the flow in a tidal channel with regard to the variation in time and the bed roughness.

2.2 Normalization

The results of the computations using the various turbulence models are given in a non-dimensional form. To this end vertical coordinates are normalized with the flow depth, h. Time is scaled with the tidal period, T_p, and velocities are scaled with a friction velocity. A friction velocity u_* is defined by

$$u_* = \sqrt{\tau_0} \tag{11}$$

where τ_0 is the bed shear stress.
The friction velocity used to scale the velocities, u_{*s}, is the friction velocity applying in a steady flow, with as a pressure gradient S, the amplitude of the varying pressure gradient (see equation 9). A simple momentum balance gives

$$u_{*s} = \sqrt{\tau_{0s}} = \sqrt{Sh} \tag{12}$$

where τ_{0s} is the bed shear stress in the steady flow situation.

The normalized quantities, denoted by the suffix +, read

$$z^+ = \frac{z}{h} \tag{13}$$

$$t^+ = \frac{t}{T_p} \tag{14}$$

$$u^+ = \frac{u}{u_{*s}} = \frac{u}{\sqrt{Sh}} \tag{15}$$

$$\nu_t^+ = \frac{\nu_t}{\sqrt{Sh^3}} \tag{16}$$

Equations (7) and (10) read in the normalized form

$$\tau^+ = -\nu_t^+ \frac{\partial u^+}{\partial z^+} \tag{17}$$

and

$$R \frac{\partial u^+}{\partial t^+} - \frac{\partial}{\partial z^+}(\nu_t^+ \frac{\partial u^+}{\partial z^+}) = \cos (2\pi\ t^+) \tag{18}$$

where

$$R = \frac{\sqrt{h}}{T_p \sqrt{S}} \quad . \tag{19}$$

Substitution of equation (19) in equation (12) leads to an expression for u_{*s} depending on R instead of S

$$u_{*s} = \frac{h}{RT_p} \tag{20}$$

In all computations with the various turbulence models the same value for R is used: $R = 6.07 \times 10^{-3}$. With $T_p = 4.41 \times 10^4$s (12 hours and 25 minutes) this value leads for different channel depths to the friction velocities for steady flow as given by table 1. In this table a depth-averaged velocity for the steady flow, $u_{av,s}$, is also given. This depth-averaged velocity applies for $C = 60\ m^{\frac{1}{2}}/s$. C, the Chézy resistance coefficient depends on the ratio of the depth-averaged velocity, u_{av}, and the friction velocity, u_*. It is defined by

$$C = \frac{u_{av}}{u_*} g^{\frac{1}{2}} \tag{21}$$

h	u_{*s}	$u_{av,s}$
5 m	0.0187 m/s	0.358 m/s
10 m	0.0374 m/s	0.715 m/s
15 m	0.0560 m/s	1.073 m/s
20 m	0.0748 m/s	1.430 m/s

table 1

Flow situations with the same R and corresponding normalized boundary (and initial) conditions yield the same normalized solution.

2.3 Logarithmic Velocity Profiles

As discussed in Booij (1981a)most measurements in tidal flows show almost logarithmic velocity profiles, except at slack water (see Bowden et al., 1959).

A logarithmic velocity profile above a rough bed can be described by

$$u(z) = \frac{u_*}{\kappa} \ln \left(\frac{z+z_0}{z_0}\right) \tag{22}$$

where z_0 is the characteristic roughness height and κ is the Von Karman constant. Neglect of z_0 compared to z and division of equation (22) by u_* gives

$$\frac{u(z)}{u_*} = \frac{1}{\kappa} \ln \left(\frac{z}{z_0}\right) \tag{23}$$

or normalized

$$\frac{u^+(z^+)}{u_*^+} = \frac{1}{\kappa} \ln \left(\frac{z^+}{z_0^+}\right) \tag{24}$$

The depth-average of equation (23) reads

$$\frac{u_{av}}{u_*} = \frac{1}{\kappa} \{\ln (\frac{h}{z_0}) - 1\} \tag{25}$$

In tidal channels the relative characteristic roughness height z_0/h is found to be mostly between (see e.g. Sternberg, 1968, and Booij, 1981a)

$$\frac{z_0}{h} = z_0^+ = 0.001 \quad \text{and} \quad = 0.0001 \tag{26}$$

Equation (25) leads for these values of z_0^+ to

$$\frac{u_{av}}{u_*} = \frac{u_{av}^+}{u_*^+} \simeq 14.8 \quad \text{to} \quad 20.5 \tag{27}$$

The corresponding values of the Chézy resistance coefficient are

$$C \simeq 46 \quad \text{to} \quad 64 \tag{28}$$

In the computations the values $z_0^+ = 0.001$ and $z_0^+ = 0.0001$ are used. In figure 2 the velocity profiles for both roughness values are given.

Logarithmic velocity profiles especially appear, at least to a good approximation, in uniform and steady flows under influence of a free surface slope. The shear stress profiles for these flows follow from equation (6). A kinematic pressure gradient S gives

$$\tau = \tau_0 \ (1 - \frac{z}{h}) = Sh \ (1 - \frac{z}{h}) \tag{29}$$

Equation (7), with the expression (23) substituted for u(z), then gives the parabolic eddy viscosity distribution.

$$\nu_t = \kappa u_* \ z(1 - \frac{z}{h}) \qquad \left(\nu_t^+ = \kappa u_*^+ \ z^+(1 - z^+) \right) \tag{30}$$

with u_* in this steady flow given by

$$u_{*} = u_{*s} = \sqrt{Sh} \tag{31}$$

In tidal flow the term accounting for the time dependence of u in the momentum equation (equation(10) or (18)) is negligible at near maximum velocities. In that part of the tidal period the first part of equation (29) and equation (30) still apply. As the velocity and the shear stress, however, do not have to be in phase with the pressure gradient (see chapter 4), τ_0 and u_* may be smaller than the values applying for steady flow at S the maximum pressure gradient, Sh and $\sqrt{Sh}$ respectively.

At smaller velocities the time dependence of u may be important. Equations (29) and (30) then do not have to hold good.

At the two roughness values, used, only the eddy viscosity near the bed is really important for the depth-averaged velocity u_{av}. The velocity at z/h = 0.1 is in both cases already about 80% of u_{av}. Not too drastic changes in the eddy viscosity distribution farther from the bed only result in minor changes in the velocity profile.

In chapter (4) some attention is given to the consequences of different for R en z_0 on the results of the computations. Only cases without a nett discharge over the tidal cycle are considered, because the tidal average of the imposed pressure gradient is taken zero.

3 Turbulence Models

3.1 Eddy Viscosity Models

All models considered in this report are of the eddy viscosity type. The kinematic shear stress τ is, following a suggestion by Boussinesq (1877), equated to a product of the velocity gradient and a coefficient, the so called kinematic eddy viscosity. On dimensional grounds the eddy viscosity can be written as the product of a length scale, L_t, and a velocity scale, V_t.

$$\nu_t = L_t V_t \qquad \left(\nu_t^+ = L_t^+ V_t^+\right) \tag{32}$$

The models can be classified in two groups

- models in which the velocity scale is expressed in main flow quantities. (The simple eddy viscosity models and the mixing-length model)
- models in which the velocity scale is expressed in turbulence quantities. (The k-model and the k-ε-model).

The length scale is often prescribed. In the k-ε-model the length scale is expressed in turbulence quantities.

3.1.1 Simple eddy viscosity models

In the simple eddy viscosity models L_t and V_t are expressed in main flow quantities. Booij (1981a)devotes much attention to this kind of models. Models where V_t is the shear stress velocity u_* or the depth-averaged velocity u_{av} and L_t is a parabolic function of z are preferred. In this report is used

$$L_t = \kappa z\left(1 - \frac{z}{h}\right) \qquad \left(L_t^+ = \kappa z^+(1-z^+)\right) \tag{33}$$

and

$$V_t = u_* \qquad \left(V_t^+ = u_*^+\right) \tag{34}$$

Using these values ν_t behaves in accordance with formula (30). The model is exact, when logarithmic velocity profiles and linear shear stress distributions

apply. Results obtained with the model around slack water are less reliable. Models of this kind lack general applicability and need ad hoc adjustments of the viscosity for different problems. (Launder and Spalding, 1972).

3.1.2 Mixing-length model

Prandtl's (1925) mixing length hypothesis is based upon a description of the transport of momentum in boundary layer flow across the main flow direction. The used length and velocity scales are

$$L_t = l_m \qquad \left(L_t^+ = l_m^+\right) \tag{35}$$

and

$$V_t = l_m \left|\frac{\partial u}{\partial z}\right| \qquad \left(V_t^+ = l_m^+ \left|\frac{\partial u^+}{\partial z^+}\right|\right) \tag{36}$$

where l_m the mixing-length must be specified. Often a mixing-length is used that is proportional to z near the bed and is constant in the upper part of the flow. This distribution originates from boundary layer considerations without a free surface. The mixing length will most likely decrease again near the free surface (Ellison, 1960).

The similarity hypothesis of Von Karman (1930) presents a method to calculate a mixing-length.

$$l_m = \left| \frac{\partial u/\partial z}{\partial^2 u/\partial z^2} \right| \tag{37}$$

Unfortunately the obtained mixing-length is not always in agreement with measurements. Computational problems arise at inflexion points of the velocity profile, so this hypothesis is not appropriate in tidal flow. In a steady free surface flow in a channel this problem does not arise. The similarity hypothesis leads to

$$l_m = 2\,\kappa h\,(1 - \frac{z}{h})^{\frac{1}{2}}\,\{1 - (1 - \frac{z}{h})^{\frac{1}{2}}\} \qquad (38)$$

and velocity profiles that deviate slightly from logarithmic profiles. The Bakhmetev approximation of expression (38) (see fig. 3)

$$l_m = \kappa z\,(1 - \frac{z}{h})^{\frac{1}{2}} \qquad \left(l_m^+ = \kappa z^+ (1-z^+)^{\frac{1}{2}}\right) \qquad (39)$$

leads to exact logarithmic velocity profiles. In the mixing-length model, used in this report, V_t and L_t are chosen according to the equations (35), (36) and (39).

The mixing-length model is to be recommended for simple boundary layer flows (Rodi, 1980). The model is less reliable at slack water, as the mixing-length is probably not independent of the velocity profile. A disadvantage of the mixing-length model is that turbulence transport is left out of account. In problems with a considerable turbulence transport, the turbulence level and in this connection the momentum transport and the eddy viscosity can be influenced. The mixing-length hypothesis is not appropriate in that case.

3.1.3 k-Model

The coefficient for eddy diffusion in a homogeneous flow field D_t can be written (see Hinze, 1975)

$$D_t = \sqrt{\overline{u_3'^2}}\,\Lambda_L \qquad (40)$$

where the velocity scale, $\sqrt{\overline{u_3'^2}}$, is the intensity of the z component, u_3', of the turbulent velocity and the length scale is the Lagrangian integral length scale Λ_L. Prandtl (1945) and Kolmogorov (1942) proposed a related expression for the eddy viscosity to be valid more generally

$$\nu_t = C_\nu \sqrt{k}\, L \qquad (41)$$

The velocity scale chosen is

$$V_t = \sqrt{k} \qquad (42)$$

where k is the mean kinematic turbulence kinetic energy

$$k = \tfrac{1}{2}(\overline{u_1'^2} + \overline{u_2'^2} + \overline{u_3'^2}) \tag{43}$$

u_1' and u_2' are the other components of the turbulent velocities. The length scale L is like Λ_L and l_m a characteristic length scale of the more energetic turbulent eddies. L is closely related to l_m and it is in this report identified with it. The constant C_ν depends on the choice of L. (see page 26).

Determining the turbulence energy by a transport equation makes the k-model more appropriate than the mixing-length model when turbulence transport is considerable. The exact turbulence energy transport equation, based upon the Navier-Stokes equation, reads, using the eddy viscosity hypothesis (see equation 7), (Bradshaw et al., 1981; Launder and Spalding, 1972)

$$\frac{Dk}{Dt} = + \nu_t \left(\frac{\partial u}{\partial z}\right)^2 - \frac{\partial}{\partial z}\left(\overline{u_3'k'} + \overline{u_3'p'}\right) - \nu \sum_{i,j} \overline{\left(\frac{\partial u_i'}{\partial x_j}\right)^2} \tag{44}$$

where k' and p' are turbulent fluctuations of the kinematic turbulence energy and pressure; x_j are the three coordinates x, y and z, and ν is the molecular viscosity. In the k-model the diffusion is assumed to be proportional to the gradient of k, and the diffusion coefficient to be proportional to the eddy viscosity with a constant factor $1/\sigma_k$

$$-\left(\overline{u_3'k'} + \overline{u_3'p'}\right) = \frac{\nu_t}{\sigma_k}\frac{\partial k}{\partial z} \tag{45}$$

The dissipation occurs predominantly in the smallest eddy sizes, but the dissipation rate is controlled by the energy transfer from larger to smaller eddies. This cascade process is supposed to be only dependent on k and L. For dimensional consistency the dissipation term reads

$$-\nu \sum_{i,j} \overline{\left(\frac{\partial u_i'}{\partial x_j}\right)^2} = C_D \frac{k^{3/2}}{L} \tag{46}$$

The consideration above is only possible for large Reynolds numbers, in order that a range of eddy sizes occurs, where the cascade process takes place. Large Reynolds numbers are required too to get local isotropy at the small eddy sizes. This local isotropy makes it possible to express the dissipation as a single scalar quantity, ε. An objection that can be raised against expression (46) is, that the scale L and the eddy sizes of the energy containing eddies, are above the cascade range, for which range the argument given was valid.

Replacing again the Stokes derivative by the time derivative the turbulence energy transport equation (44) becomes, after substituting equations (45) and (46)

$$\frac{\partial k}{\partial t} = \nu_t \left(\frac{\partial u}{\partial z}\right)^2 + \frac{\partial}{\partial z}\left(\frac{\nu_t}{\sigma_k}\frac{\partial k}{\partial z}\right) - C_D \frac{k^{3/2}}{L} \tag{47}$$

The constants C_D and σ_k have to be chosen in such a way that the measured energy profiles are reproduced best. (See 3.3).

To normalize equation (47) the turbulence energy is scaled by Sh

$$k^+ = \frac{k}{Sh} \tag{48}$$

Equation (47) and expression (41) read normalized

$$R\frac{\partial k^+}{\partial t^+} = \nu_t^+ \left(\frac{\partial u^+}{\partial z^+}\right)^2 + \frac{\partial}{\partial z^+}\left(\frac{\nu_t^+}{\sigma_k}\frac{\partial k^+}{\partial z^+}\right) - C_D \frac{k^{+3/2}}{L^+} \tag{49}$$

and

$$\nu_t^+ = C_\nu \sqrt{k^+}\, L^+ \tag{50}$$

Drawbacks of the k-model are the weak basis on which equations (41), (45) and (46) rest. A length scale distribution has still to be specified. It is risky to use the model for situations where no reliable measurements are present. In this report such a situation is the tidal phase around slack water.

3.1.4 k-ε-model

In many flow problems the length scale distribution is hard to prescribe, e.g. in tidal flow around slack water. To remove this difficulty several transport equations for different combinations of k and L are proposed (Launder and Spalding, 1972). Most succesfull up to now is the equation for $\epsilon = C_D\, k^{3/2}/L$. In the k-ε-model two equations, the transport equation for k and ε, are needed to calculate the eddy viscosity. In this model the eddy viscosity is written

$$\nu_t = C_1 \frac{k^2}{\epsilon} \tag{51}$$

where

$$C_1 = C_\nu C_D \tag{52}$$

The velocity scale in the eddy viscosity is still $\sqrt{k}$. The length scale is

$$L_t = C_D \frac{k^{3/2}}{\epsilon} \tag{53}$$

The k-equation becomes

$$\frac{\partial k}{\partial t} = C_1 \frac{k^2}{\epsilon} \left(\frac{\partial u}{\partial z}\right)^2 + \frac{C_1}{\sigma_k} \frac{\partial}{\partial z} \left(\frac{k^2}{\epsilon} \frac{\partial k}{\partial z}\right) - \epsilon \tag{54}$$

The ε-equation used reads

$$\frac{\partial \epsilon}{\partial t} = C_{p\epsilon}\, k \left(\frac{\partial u}{\partial z}\right)^2 + \frac{C_1}{\sigma_\epsilon} \frac{\partial}{\partial z} \left(\frac{k^2}{\epsilon} \frac{\partial \epsilon}{\partial z}\right) - C_{d\epsilon} \frac{\epsilon^2}{k} \tag{55}$$

Equation (55) is the equation generally used.(for this case the Stokes derivative is again replaced by the time derivative.) This ε-equation is related to an exact equation based on the Navier-Stokes equatuon, but the assumptions in equation (55) are so far-reaching that it is more appropriate to call equation (55) an empirical equation (Bradshaw et al., 1981). The diffusion term in particular represents a combination of different terms, which are not easily simplified on theoretical grounds. So the following relation is assumed in which the theoretical terms on the right side are related to a diffusion term in analogy with the diffusion term in the k-equation (47).

$$-\frac{C_1}{\sigma_\varepsilon}\frac{\partial}{\partial z}\left(\frac{k^2}{\varepsilon}\frac{\partial \varepsilon}{\partial z}\right)=\sum_{i,j,k}\left[\overline{\frac{\partial u_j'}{\partial x_k}\frac{\partial u_i'}{\partial x_k}\frac{\partial u_i'}{\partial x_j}}+\overline{u_j'\frac{\partial}{\partial x_j}\left\{\tfrac{1}{2}\left(\frac{\partial u_i'}{x_k}\right)^2\right\}}+\overline{\frac{\partial u_i'}{\partial x_k}\frac{\partial^2 p'}{\partial x_k \partial x_i}}\right] \tag{56}$$

The diffusion term is again assumed to be proportional to the gradient of ε, with a diffusion coefficient that is proportional to the eddy viscosity with a constant factor $1/\sigma_\varepsilon$. The only justification stemms from the various flow situations described reasonably well with the k-ε-model.(see Rodi, 1980)

To normalize the equations of the k-ε-model ε is scaled by $\sqrt{S^3 h}$

$$\varepsilon^+ = \frac{\varepsilon}{\sqrt{S^3 h}} \tag{57}$$

The normalized versions of equations (51), (54) and (55) read

$$\nu_t^+ = C_1 \frac{k^{+2}}{\varepsilon^+} \tag{58}$$

$$R\frac{\partial k^+}{\partial t^+} = C_1 \frac{k^{+2}}{\varepsilon^+}\left(\frac{\partial u^+}{\partial z^+}\right)^2 + \frac{C_1}{\sigma_k}\frac{\partial}{\partial z^+}\left(\frac{k^{+2}}{\varepsilon^+}\frac{\partial k^+}{\partial z^+}\right) - \varepsilon^+ \tag{59}$$

and

$$R\frac{\partial \varepsilon^+}{\partial t^+} = C_{p\varepsilon} k^+ \left(\frac{\partial u^+}{\partial z^+}\right)^2 + \frac{C_1}{\sigma_\varepsilon}\frac{\partial}{\partial z^+}\left(\frac{k^{+2}}{\varepsilon^+}\frac{\partial \varepsilon^+}{\partial z^+}\right) - C_{d\varepsilon}\frac{\varepsilon^{+2}}{k^+} \tag{60}$$

The constants $C_{p\varepsilon}$, $C_{d\varepsilon}$ and σ_ε have to be specified by calibration in situations where extra conditions concerning the dissipation can be imposed.
The empirical nature of the ε-transport equation requires great care in using the k-ε-model for flow problems lacking a sufficient body of empirical evidence.

3.2 Boundary Conditions

To solve the differential transport equations of the models introduced

above, appropriate boundary conditions have to be imposed. For each differential equation a boundary condition is specified near the bed and one at the free surface

Bed boundary conditions

u: The lowermost grid point is chosen in the logarithmic part of the velocity profile. Generally a logarithmic velocity profile is assumed in the region $30 < z^* < 100$ where z^* is a dimensionless wall distance (The law of the wall, see Townsend, 1976)

$$z^* = \frac{z u_*}{\nu} \tag{61}$$

with ν the kinematic molecular viscosity. The region in which the velocity profiles are logarithmic in the problem considered in this report, extends to much larger distances from the wall. Using $z^* < 100$ for the first grid point, corresponding with $z^+ < 0.0025$ when using for u_* the values of table 1, would require much larger computing times (see 4.2). The boundary condition for the velocity used is chosen conform to equation (24)

$$u^+(z^+) = \frac{u^+}{\kappa} \ln\left(\frac{z^+}{z_0^+}\right) \tag{62}$$

k: In the transport equation (equation 49) for the turbulence energy the terms accounting for the time dependence and for the diffusion of k are negligible in the near-wall region, so that local equilibrium prevails. Substitution of the expressions (50), (52) and (17) in equation (49) gives the bed boundary condition for the turbulence energy

$$k^+(z^+) = \frac{1}{\sqrt{C_1}} \tau^+(z^+) \tag{63}$$

Usually the near-constancy of τ near the wall is used to approximate equation (63) by (see Rodi, 1980)

$$k^+(z^+) = \frac{1}{\sqrt{C_1}} u_*^{+2} \tag{64}$$

When a linear stress profile can be assumed, use of the normalized form of equation (29) yields the boundary condition used in this report

$$k^+(z^+) = \frac{1}{\sqrt{C_1}} u_*^{+2} (1 - z^+) \tag{65}$$

The same boundary condition for k applies in the k-ε-model. Instead of equations (49) and (50) equations (54) and (58) are now used to derive the boundary condition .

ε: The bed boundary condition for the dissipation follows from the same neglect of the time dependence term and the diffusion term in the transport equation for k (equation 54), giving

$$\varepsilon^+(z^+) = \sqrt{C_1}\, k^+ \left|\frac{\partial u^+}{\partial z^+}\right| \tag{66}$$

With $\partial u^+/\partial z^+$ from equation (62) and substitution of equation (64) the normally used bed boundary condition for the dissipation results

$$\varepsilon^+(z^+) = \frac{u_*^{+3}}{\kappa z^+} \tag{67}$$

With equation (65) the boundary condition used in this report follows

$$\varepsilon^+(z^+) = \frac{u_*^{+3}}{\kappa} \frac{(1-z^+)}{z^+} \tag{68}$$

Free surface boundary conditions

u: When no wind-induced shear stress is present at the free surface, the free surface boundary condition used is a zero u-gradient, so no momentum transport takes place across the free surface regardless of the value of the viscosity.

$$\left(\frac{\partial u^+}{\partial z^+}\right)_{z^+=1} = 0 \tag{69}$$

k: No turbulence energy transport across the free surface is assumed. This leads to an analogous free surface condition for the turbulence energy

$$\left(\frac{\partial k^+}{\partial z^+}\right)_{z^+=1} = 0 \qquad (70)$$

ε: An expression analogous to equations (69) and (70) is often used for the free surface boundary condition for ε too (see e.g. Smith and Takhar, 1979)

$$\left(\frac{\partial \varepsilon^+}{\partial z^+}\right)_{z^+=1} = 0 \qquad (71)$$

There is, however, no reason to assume that no ε can be transported through the surface. In this report the expression for the boundary condition at the surface corresponds with the boundary condition at the bed in its dependence on the turbulence energy (see Rodi, 1980)

$$(\varepsilon^+)_{z^+=1} = \frac{\{\sqrt{C_l}(k^+)_{z^+=1}\}^{3/2}}{C_{b\varepsilon}\kappa} \qquad (72)$$

The purpose of this boundary condition is to limit the length scale near the free surface. $C_{b\varepsilon}$ is a constant.

The differential equations of the various models are solved numerically by means of a fully implicit finite difference method (see appendix).
To this end the depth is divided in cells around grid points, at which u, k and ε are calculated (see appendix). Finite difference counterparts of the transport equations can be derived by a discretization of these transport equations over the cells. To keep the truncation errors caused by this discretization small, a depth grid is used with the following properties (see fig. 4):

- the spacing between the grid points is small in regions where important gradients occur (e.g. near the bed).
- the cell around the first grid point is small in comparison to the distance between this first grid point and the bed.
- the grid is moderately non-uniform. A non-uniform depth grid requires less grid points and so less computing time but strongly non-uniform depth grids cause considerable truncation errors.

The bed boundary value for the velocity is introduced by means of a momentum balance equation for the cell around the first grid point.
The time step has to be chosen small in most models for reasons of numerical stability. Therefore the results of the computational generally do not depend anymore on the time step used. (see chapter 4).

3.3 Choice of the Constants

Various constants and in some models a length-scale distribution have to be specified. The constants are determined from special flow configurations, but some fine tuning according to the problem considered is sometimes done (Launder and Spalding, 1972). In this report the values as recommended by Launder and Spalding(1972) are used (see table 2). The values chosen were the best overall values for a wide range of boundary-layer flows

constant	k-model	k-ε-model
C_l	0.08	0.09
$C_{p\varepsilon}$	-	$1.45 \times C_l = 0.130$
$C_{d\varepsilon}$	-	$0.18/C_l = 2.0$
σ_k	1.0	1.0
σ_ε	-	1.3

table 2

For the constant $C_{b\varepsilon}$ appearing in the free surface boundary value for ε (equation 72) the value 0.07 is chosen (Hossain, 1980). The length scale distribution used in the mixing-length model and in the k-model is the Bakhmetev distribution (see equation 39).

The various models and the influence of a variation of their constants are investigated first. This investigation is carried out for the case of a steady channel flow with a free surface and a normalized roughness length $z_0^+=0.001$. The behaviour of the models in the case of a tidal flow is mainly determined by the behaviour in the case of steady flow,as tidal flow can be considered a slowly varying flow (see chapter 4). It was demonstrated in chapter 2 that for $z_0^+=0.001$ the viscosity in the upper part of the flow is hardly important. The viscosity profiles computed for this steady flow are compared in fig. 5a. The differences appear mainly in the upper part of the flow. Consequently the velocity profiles of the various models in fig. 5b show only small differences.

Additional comments on the choice of the constants are given in 3.3.2 and 3.3.3.

3.3.1 Simple eddy viscosity model and mixing-length model

The eddy viscosity distribution prescribed in the simple eddy viscosity (E-V) model is the parabolic distribution. In steady channel flow with a free surface this distribution brings about a logarithmic velocity profile (see 3.1). If in the mixing-length (M-L) model the Bakhmetev distribution is chosen for the length scale, the same eddy viscosity profile and so the same logarithmic velocity distribution appear (see 3.2).

Knowledge of the mixing-length and the viscosity profile near a free surface is limited. The influence of distributions that differ in the upper part of the flow on the velocity profile is small. Deriving the mixing length and the viscosity distributions in the upper part of the flow is therefore hardly possible. The differences between computations with distributions that deviate in the upper part of the flow, however, are also small.

3.3.2 k-Model

In the equations of the k-model (equations 18, 49 and 50), the constants C_D, C_ν and σ_k and the length scale distribution have to be specified

Near the bed local equilibrium of the turbulence prevails, so equation (65) applies, C_1 in equation (65) is the product of C_ν and C_D (equation 52). Measurements of the ratio of the turbulent energy and the shear stress in experiments near walls yield $C_1^{\frac{1}{2}} \approx 0.25$ to 0.3, suggesting a value of C_1 of about 0.08 (see Launder and Spalding, 1972). The values of C_ν and C_D depend on the choice of the length scale. When the Bakhmetev distribution (equation 39) is used, at least near the bed, equations (39), (30), (50) and (65) lead to $C_\nu = C_1^{\frac{1}{4}} = 0.53$ and $C_D = C_1^{3/4} = 0.15$.

The distribution of the length scale in the k-model is as poorly known as the mixing-length. Because of the conceptual correspondence between the two length scales, they are often taken to be identical. The value of σ_k originates from measurements of Hanjalic and Launder (1972) in an asymmetric flow between two parallel planes with different roughness. The diffusion term in the k-equation is more important in this flow configuration than it is normally in wall boundary flows. The value obtained in this way is $\sigma_k = 1.0$ (Launder and Spalding, 1972).

If local equilibrium of the turbulence would prevail at every depth, the k-distribution would be linear according to equation (65). The diffusion term in equation (49) brings about a transport upwards through the flow. As a consequence the turbulence energy content in the lower half of the flow is somewhat smaller and in the upper half larger than the linear relation would predict (see fig. 6). Values of the turbulence energy estimated from measurements of some turbulence intensities in free surface flows (Atkins, 1980; Nakagawa et al., 1975) are comparable to the values computed by means of the k-model up to the surface. Variation of the constants C_1 and σ_k has only a small influence on the upper half of the viscosity profile (fig. 7) and hardly any on the velocity profile (table 3). The same applies for other choices of the length scale distribution.

	$(u^+)_{z^+=1}$
$\sigma_k = 1$; $C_1 = 0.08$	16.98
σ_k x 2	17.02
C_1 x 4	17.02

table 3

The values of the constants used by Smith and Takhar (1979) in their k-model computation of long wave flow deviate from the values usually accepted: C_1=0.4 and C_ν=1.78 (Smith and Takhar, 1978). The length scale adopted by Smith and Takhar is approximately the mixing-length in the near-bed region. Close to the surface a constant length scale is used. With these values of C_1, C_ν and L^+ the viscosity near the bed is 2.4 times the value agreeing with the logarithmic profile as given by equation (30).
Smith and Takhar have obviously used the constants of the k-model for tuning the model, without giving due attention to all conditions that have to be fullfilled.

3.3.3 k-ε-Model

In the equations of the k-ε-model (equations 18, 58, 59 and 60) many constants have to be specified C_1, $C_{p\varepsilon}$, $C_{d\varepsilon}$, σ_k, σ_ε and in the free surface boundary condition for ε (equation 72): $C_{b\varepsilon}$.
Local equilibrium near the bed gives again equation (63), and hence $C_1 \simeq 0.08$. Experiments on the decay of turbulence behind a grid yield $C_{d\varepsilon} \simeq 2.0$. (See Launder and Spalding, 1972). To provide a value for $C_{p\varepsilon}$. equilibrium of the dissipation near the bed is considered. The production of ε in the ε-transport equation (60) can be related to the production of turbulence energy, which near the bed approximately equals the energy dissipation

$$C_{p\varepsilon}\, k^+ \left(\frac{\partial u^+}{\partial z^+}\right)^2 = C_1 \frac{k^{+2}}{\varepsilon^+} \left(\frac{\partial u^+}{\partial z^+}\right)^2 \times \frac{C_{p\varepsilon}}{C_1} \frac{\varepsilon^+}{k^+} \simeq \frac{C_{p\varepsilon}}{C_1} \frac{\varepsilon^{+2}}{k^+} \tag{73}$$

Substitution of equation (73) in the time-independent form of equation (60) gives for near wall flow

$$\left(\frac{C_{p\varepsilon}}{C_1} - C_{d\varepsilon}\right) \frac{\varepsilon^{+2}}{k^+} + \frac{C_1}{\sigma_\varepsilon} \frac{\partial}{\partial z^+} \left(\frac{k^{+2}}{\varepsilon^+} \frac{\partial \varepsilon^+}{\partial z^+}\right) = 0 \tag{74}$$

Rewriting of this equation by means of the expressions (65) and (68), both applying for the near-wall region, yields

$$\frac{C_{p\varepsilon}}{C_1} - C_{d\varepsilon} + \frac{\kappa^2}{\sigma_\varepsilon \sqrt{C_1}} = 0 \tag{75}$$

When the Reynolds analogy for the diffusion of momentum, turbulence energy and dissipation, meaning $\sigma_k = 1$ and $\sigma_\varepsilon = 1$, is used, equation (75) yields $C_{p\varepsilon} = 0.114$.

The values of the constants determined above do not have a firm base, as the physical background of the k-ε-model, including the assumption of the Reynolds analogy, is limited. The values in table 2, recommended by Launder and Spalding (1972) and used in this report, provide good overall values for a wide range of boundary layer flows. The constants, however, do not satisfy equation (75) any more. This means that the diffusion of ε is not correctly described in the ε-

transport equation. When the diffusion near the bed is correctly treated, satisfying equation (75), then the diffusion farther from the bed is not reproduced rightly. Using the values of table 2, the contribution of the diffusion of ε is decreased, lessening ε and increasing L (fig. 8a) and ν_t above the bed region. Actually if one or more of the constants would vary over the depth a better but less useful model would be obtained.

The necessary correction on the values of the constants that satisfy equation (75) depends on the flow configuration. Much empirical information is required for the tuning of the constants for a certain problem. The obtained values are not always useful in other situations. Concerning the problem, considered in this report, a calibration can be executed for steady flow. This calibration will be satisfactory in tidal flow in the tidal phases where the velocity profile is approximately logarithmic. In tidal phases where the velocity profile is not logarithmic different tunings would possibly have preference. For this reason the computations are executed with the broadly applicable values of table 2.

Small changes in the tuning can have important consequences as the first two terms of equation(75) are much larger than the third term. Small changes in $C_{d\varepsilon}$ or $C_{p\varepsilon}$ result in relatively large changes of the contribution of the diffusion term in the ε-transport equation.

Variation of the free surface boundary condition of ε has an important influence on the length scale distribution in the upper part of the flow (see fig. 8b). In case of a zero-gradient boundary condition as used by e.g. Smith and Takhar (1979) the maximum length scale and the maximum eddy viscosity lie at the surface. The dependence of the turbulence energy and of the velocity at the surface on the free surface boundary condition of ε are appreciable in the steady flow situation as considered in this chapter (see table 4). Experimental information about the behaviour of the length scale and other turbulence quantities is scarse. Relation (72) and the value $C_{b\varepsilon}=0.07$ are only tentative (Rodi, 1980).

boundary condition	$(k^+)_{z^+=1}$	$(u^+)_{z^+=1}$
$C_{b\varepsilon} = 0.35$	0.358	17.34
$C_{b\varepsilon} = 0.07$	0.528	17.27
$C_{b\varepsilon} = 0.014$	0.853	16.99
$(\partial\varepsilon^+/\partial z^+)_{z^+=1} = 0$	0.981	16.87

table 4

3.4 Comparison of the Turbulence Models

The performances of the various turbulence models, discussed above, are compared for the steady free surface channel flow of (3.3).

The 4 models discussed (E-V, M-L, k-model and k-ε-model) give approximately the same velocity profiles (fig. 5b), corresponding with approximately equal eddy viscosities in the lower half of the flow (fig. 5a). Only the k-ε-model gives somewhat smaller viscosities in the lower half of the flow and somewhat higher velocities, while tuning of this model for this exact problem is not executed. The small difference between the k-profiles of the k-model and the k-ε-model computations is caused by the different values of C_1 used. E.g. using C_1=0.09, the k-model yields the k-profile of the k-ε-model. The simple eddy viscosity model and the mixing length model give identical results when the eddy viscosity distribution is parabolic and the length-scale has the Bakhmetev distribution. The k-model, using the Bakhmetev length scale distribution shows only small deviations of the velocity near the surface and for $z^+ \approx 0.25$. The deviations are caused by the diffusion of turbulence energy. The k-ε-model can be tuned to yield the logarithmic profile of the E-V and the M-L models by changing σ_ε, $C_{d\varepsilon}$ or $C_{p\varepsilon}$. The influence of this tuning on the surface velocity is important (see table 5).

model		$(u^+)_{z^+=1}$
E.V-model		17.14
k-model		16.98
k-ε-model	$\sigma_\varepsilon = 1.2$	17.07
	$\sigma_\varepsilon = 1.3$	17.24
	$\sigma_\varepsilon = 1.4$	17.49
	$C_{p\varepsilon} = 1.39$	16.98

table 5

The k-ε-model tuned with e.g. $C_{p\varepsilon}$=1.39 yields a length scale distribution close to the Bakhmetev-distribution (fig. 8c). The eddy viscosity distribution and the velocity distribution agree closely with the results of the k-model.

The small relative roughness z_0^+ in the considered flow configuration conceals possible differences between the various models, as the velocity distribution is determined mainly by the eddy viscosity near the bed in this case. Diffusion of turbulence energy is hardly important near the bed and the ε-transport equation yields practically the Bakhmetev-distribution near the bed, so the eddy viscosity is equal there in all models used.

For steady flow configurations with a small relative roughness, e.g. flow in rivers and channels, the k-ε-model (and the k-model) seem to be usefull only in some special cases all connected with non-logarithmic velocity profiles. The determination of the length scale distribution is difficult in density-layered flow, around dunes on the river bed and along steep channel and river banks, especially when the channel is strongly curved. The k-ε-model can provide length scale distributions in those cases. In density-layered flow the problem is more complex still, as the constants in the k-model and the k-ε-model depend on the density gradient. (See Rodi, 1980) Convection of k and ε is generally negligible in rivers, etc. because of the short adjustment times of k and ε (see chapter 4).

In non-steady flow configurations the k-model or the k-ε-model may be the suitable turbulence model if the term accounting for the time dependence in the transport equation of k or ε cannot be neglected. (see chapter 4).

4. Tidal Flow

4.1 Computation of Tidal Flow with Different Turbulence Models

The four turbulence models of (3.1) are used to compute the velocities and shear stresses in tidal flow in the situation of (2.2)($R=6.07\times10^{-3}$) for 2 characteristic roughness heights $z_0^+=0.001$ and $z_0^+=0.0001$. Again for simplicity the one dimensional flow model of (2.1) is used. The depth grid is given in fig. 4.

The development of the velocity profiles over the tidal cycle for $z_0^+=0.001$, computed by means of the four turbulence models, are presented in fig.10. The tidal period is divided in 24 equal parts, during about half an hour each. Zero is the mark of the phase of maximum surface slope or maximum pressure gradient. The time step used is 1/2400 tidal period as this was the largest time step allowed by the k-ε-model in this case. The velocities computed with the k-ε-model are generally 1% higher than those computed with the other models. This difference is connected with the constants used in the model. The shape of the profiles at near maximum velocities closely follow the profiles computed in steady flow (fig. 5b). The pressure gradient in the steady flow computation is taken equal to the amplitude of the varying pressure gradient in tidal flow. The maximum velocity in the tidal flow, however, is smaller than the velocity in steady flow, as this maximum velocity takes place about 50 minutes after the maximum pressure gradient.

The differences between the velocity profiles computed by means of the various turbulence models are negligible. Even at slack water the differences are small. They amount to time differences of at most about 3 minutes or 1½ degree. Also the time difference between zero velocity near the bed and near the surface can differ from model to model, but the differences between the models are at most about 3 minutes.

The differences between the velocity profiles are connected with the differences in the eddy viscosity profiles in the various models. These are given in figure 11. The profiles at maximum velocity again closely resemble the viscosity profiles in case of steady flow (see fig. 5a). Near slack water the viscosity profiles differ slightly, bringing about differences of the velocity profiles too. As was discussed in chapter 3 all 4 models may be less precise near slack water. The dip at slack water in the viscosity profile computed with the mixing length hypothesis is caused by a zero-velocity gradient at that point.

The flow at the higher velocities approximates steady flow, as is shown by the correspondences between the velocity profiles of steady flow and tidal flow and between the eddy viscosity profiles of the two flows. The shear stress profiles in fig. 12 satisfy for the higher velocities a linear dependence on depth conforming to a steady flow situation. Only the shear stress profiles computed with the k-ε-model are shown. The other models yield shear stress profiles that differ only slightly at slack water.

In the momentum balance equation (18) the rate of change term can be compared to the production term to examine if it can be neglected. As $R \simeq 6\times10^{-3}$ and the maximum value of u^+ is about 17, comparison of the maximum value of the rate of change term and the maximum value of the production term gives

$$\left(R \frac{\partial u^+}{\partial t^+}\right)_{max} : \quad (\cos 2\pi t^+)_{max} \simeq 0.6 : 1 \qquad (76)$$

where the suffix max stands for the maximum value over the tidal period. Near the bed u^+ is smaller and consequently the rate of change term too. $\partial u^+/\partial t^+$ and $\cos 2\pi t^+$ both vary over the tidal cycle. At phases with a high velocity, the production is high too, while $\partial u^+/\partial t^+$ is small. So at the higher velocities the rate of change term can be neglected. At other phases this neglect is not correct.

An analogous consideration can be used for the rate of change terms compared to the production terms in the transport equations of k and ε (equation (49) or (59) and equation (60) respectively)

$$\left(R\frac{\partial k^+}{\partial t^+}\right)_{max} : \left(\frac{\tau^{+2}}{\nu_t^+}\right)_{max} \simeq 0.24\left(u_*^{+2}\right)_{max}(1 - z^+) : 2.5\left(u_*^{+3}\right)_{max}\frac{1-z^+}{Z^+}$$

$$\simeq 0.1\ z^+ : 1 \qquad (77)$$

and

$$\left(R\frac{\partial \varepsilon^+}{\partial t^+}\right)_{max} : \frac{C_{p\varepsilon}}{C_l}\left(\frac{\tau^{+2}}{\nu_t^+}\cdot\frac{\varepsilon^+}{k^+}\right)_{max} \simeq 0.07\left(\varepsilon^+\right)_{max} : 1.1\frac{\left(u_*^+\varepsilon^+\right)_{max}}{z^+}$$

$$\simeq 0.07\ z^+ : 1 \qquad (78)$$

Strictly speaking equations (77) and (78) do not apply near the surface. The approximation of k^+ used does not hold there. Near the surface the rate of change term has to be compared rather with the dissipation term in each equation. The result will not be much different from equations (77) en (78). Comparison of equations (76), (77) and (78) shows that the rate of change terms in the transport equations of ε and k can safely be neglected if the corresponding term in the momentum balance equation is negligible. This means that over a large part of the tidal cycle the almost logarithmic profiles of fig. 5, the k-distribution of fig. 6, etc. of the steady flow are approximated. The magnitudes deviate, however, as the pressure gradient varies, and its value differs mostly from the pressure gradient assumed in steady flow. In fig. 13 the k-profiles computed with the k-ε-model are plotted. The k-profiles computed with the k-model differ hardly.

The pressure gradient should have no influence on the length scale distribution. The length scale profiles, indeed, vary hardly, except for a short period around slack water (see fig. 14). Generally the profile of the length scale in steady flow is followed. Figure 14 shows that except for the period around slack water, the k-model and the k-ε-model will give exactly the same results if the length

scale distribution of the k-ε-model for steady flow is used.

The basis for this behaviour of the k-ε-model is the short adjustment time of k and ε when k or ε have values that do not entirely agree with the velocity gradient. If in equations (77) and (78) the τ^+ is changed slightly, large values for $\partial k^+/\partial t^+$ and $\partial \varepsilon^+/\partial t^+$ arise, restoring the balance in a short time.

Computations with the other bed roughness $z_0^+=0.0001$ yield similar results. The relative importance of the eddy viscosity in the upper part of the flow is somewhat smaller even. $\partial u^+/\partial z^+$ for logarithmic velocity profiles does not depend on z_0, so for steady flow the solutions with all four models are exactly the same as in the case of $z_0^+=0.001$ except for the velocities, to which a constant velocity is added. In the tidal phase around slack water, where logarithmic velocity distributions do not apply any more, differences between the computations with the two roughness values occur in several quantities, e.g. in the length scale. In fig. 15 some results of the k-ε-model for $z_0^+=0.0001$ are plotted. Comparison with figures 10 to 14 shows differences around slack water and in the accelerating phase, due to the larger phase lag. L^+ hardly differs.

Occasional higher values of z_0^+ in tidal flow lead to larger differences between the various models. The increased importance of the bed shear stress results in smaller phase lags.

Smith and Takhar (1977, 1979) calculated a length scale distribution using a k-ε-model for a case of free surface channel flow under long waves. The distribution calculated shows values near the channel bed that are about three times as large as the value theoretically derived, yielding much too high eddy viscosities (see fig. 16). This result casts serious doubts on their exact elaboration of the k-ε-model.

4.2 Time Step and Instability

The time step, Δt, needed in the various models to avoid instability is very different. The models using more differential equations need shorter time-steps to provide stability. As the computing time is more or less proportional to the number of differential equations used and inversely proportional to the time steps used, more complex models will need much more computing time.

In table 6 the minimum number of time steps in a tidal cycle, N, as needed in the various models in this investigation is given. Mostly the first grid point was at $z^+=0.025$.

Model	1st grid point	N(minimum for stability)
E-V	$z_0^+ = 0.025$	always stable
M-L	$z_0^+ = 0.025$	360
k-model	$z_0^+ = 0.025$	96 to 240
k-model	$z_0^+ = 0.1$	96
k-ε-model	$z_0^+ = 0.025$	2400
k-ε-model	$z_0^+ = 0.1$	720

table 6

The E-V-model was stable for all time steps used (down to N=6). The velocity profiles remained good down to N=6 except for minor effects near slack water, but the precision of the time-dependence was about proportional to Δt. The error in the time-dependence is dependent on the exact elaboration of the E-V-model. In this investigation it was about 1/10 Δt. A minimum number of N=12 to 48 is recommended depending on the precision wanted. The k-model was just stable at N=96, but on this verge of stability serious deviations near the bed occurred.

The k-model and the k-ε-model generally get instable when the time step is so large that near the bed the dissipation or the turbulence energy becomes negative. A measure of the verge of instability is the reproduction time of the turbulence energy or of the dissipation, defined by the minimum ratio of the quantity considered and its production.

The reproduction time of a quantity is the time needed by the production terms to produce the same amount of the quantity as is present. So in a steady state the quantity is completely replaced in this reproduction time on an average. The normalized reproduction time of ε and k can be estimated at (see equations 77 and 78).

$$T_k^+ = \left(R \frac{k^+}{\text{production } k^+}\right)_{min} = \left(\frac{k^+ R}{\tau^{+2}/\nu_t^+}\right)_{min}$$

$$\simeq C_1^{-\frac{1}{2}} R \kappa \left(\frac{z^+}{u^+}\right)_{min} \simeq 8.0 \times 10^{-3} z^+_{min} \qquad (79)$$

and

$$T_\varepsilon^+ = \left(R \frac{\varepsilon^+}{\text{production } \varepsilon^+}\right)_{min} = \frac{C_1}{C_{p\varepsilon}} \left(\frac{k^+ R}{\tau^{+2}/\nu_t^+}\right)_{min} \simeq 5.6 \times 10^{-3} z^+_{min} \qquad (80)$$

where the suffix min means the minimum value over depth and tidal cycle. For $z^+ = 0.025$ this amounts to $T_k^+ \simeq 2.0 \times 10^{-4}$ and $T_\varepsilon^+ = 1.4 \times 10^{-4}$ or $T_k \simeq 9$ sec and $T_\varepsilon \simeq 6$ sec. Values of $N \simeq 5000$ and $N \simeq 7000$ would result for the k-model and the k-ε-model respectively. When equilibrium between production and dissipation is approximated much lower values for N are allowed (see table 6), especially for the k-model. When, on the other hand, the initial values are not chosen very carefully, then the calculated values of the minimum number of steps are approximately needed.

The reproduction times of ε and k are proportional to z^+. Taking the bed-most grid point at $z^+=0.1$, lowers the number of steps needed in the k-ε-model, but not considerably in the k-model (See table 6). Using then a logarithmic depth-grid in the k-ε-model (see fig. 4) diminishes the viscosity in the upper half of the flow by about 10%. This has barely consequences for the velocity profile. To keep computing time lower a linear grid may be used (see fig. 4). The viscosity profiles in that case are severely affected, having consequences for the velocity profiles in the lower part of the flow (see fig.17). The bed shear stress computed is about 10% smaller, using this grid configuration.

The velocity profiles around slack water are influenced by the depth grid as the logarithmic part of the profiles at slack water, used in the boundary conditions, may not extend to the level of the grid point nearest to the bed.

The many time steps needed will severely limit the applicability of the k-ε-model for flows in estuaries, rivers, channels, etc.

4.3 Discussion of Some Results

4.3.1 Comparison with the results of Smith and Takhar

Smith and Takhar (1977, 1979) use the k-ε-model to calculate the length scale and compare it to the length scale assumed in their k-model. They are content with the similarity of the two profiles, though the ratio near the wall is 4 to 1, with important consequences for the eddy viscosity there (see fig.16). The k-ε-model in this investigation on the other hand yields a length scale distribution that approximates the Bakhmetev distribution, used in the k-model.

Rodi (1980) mentions the k-model as the optimum model in tidal flow. The computations on which this opinion is based are the k-model computations by Smith and Takhar (1979). Smith and Takhar compare their results, however, with results from two simple eddy viscosity models of Johns (1966) with improbable eddy viscosity distributions i.e. a constant eddy viscosity and a parabolic eddy viscosity with the vertex at the free surface. These models yield velocity distributions that compare badly to the logarithmic distribution found by Johns (1966). The simple eddy viscosity model of this investigation, using a parabolic eddy viscosity with the vertex at half-depth, leads also to the logarithmic velocity profiles. As the velocity profiles over the tidal cycle can hardly be distinguished from the velocity profiles computed with the k-model, the simple eddy viscosity model is generally to be preferred, considering the computation time needed.

Another point in favour of the k-model as mentioned by Smith and Takhar is the good reproduction of the phase and amplitude of the surface velocity. The k-model and the other models discussed in this report can however, hardly improve a simple depth-integrated model in this respect.

The depth-average of equation (6) reads

$$\frac{\partial u_{av}}{\partial t} = -s - \frac{\tau_0}{h} \tag{81}$$

This can be rewritten by substitution of expression (9) and equation (11) into

$$\frac{\partial u_{av}}{\partial t} + \frac{u_* |u_*|}{h} = S \cos \omega t \tag{82}$$

The friction velocity u_* can be expressed in the depth-averaged velocity u_{av} by

$$u_* = \frac{1}{\beta} u_{av} \tag{83}$$

where β is (see equations 25 and 21)

$$\beta = \frac{1}{\kappa} \{\ln(\frac{h}{z_0}) - 1\} = \frac{C}{g^{\frac{1}{2}}} \tag{84}$$

Equation (82) in normalized form is written

$$R \frac{\partial u^+_{av}}{\partial t^+} + \frac{1}{\beta^2} u^+_{av} |u^+_{av}| = \cos(2\pi t^+) \tag{85}$$

The solution of equation (85) is compared to the depth-averaged velocity computed with the E-V-model in fig. 18a. $t^+=0$ is the phase of maximum pressure gradient.
The phase of the surface velocity hardly deviates from the phase of the depth-averaged velocity as can be inferred from fig. 18b. The depth-averaged velocity appears to be equal to the velocity at $z^+=0.368 = 1/e$, even around slack water. The bed shear stress from the E-V-model and from the solution of equation (85) are compared in fig. 18c.

Equation (85) shows that the phase and the amplitude of the depth-averaged velocity, and so of the surface velocity too, depend only on β, with R given. So reproduction of these quantities is a weak criterion to evaluate the performance of a certain model.

The phase lag of the velocity with respect to the pressure gradient is smaller when the shear stress term in equation(85) is more important. Small values of β (large roughness values) or small values of R (corresponding with large pressure gradients and flow velocities) give small phase lags.

The depth grid has to be chosen with care, otherwise computational errors can be introduced. This possibly accounts for the non linear shear stress distribution mentioned by Smith and Dyer (1979), and for the deviation of τ_0 from a quadratic friction as found by Johns (1978) who used a k-model to calculate the flow in a tidal channel.

4.3.2 Phase lag of the shear stress

Not many reliable measurements of the shear stress distribution over the tidal cycle have been executed. Some measurements of tidal flow in estuaries (Gordon, 1975) and the measurements of Anwar and Atkins (1980) in a flume seem to point to an important phase lag of the shear stress with respect to the surface velocity, the so called hysteresis effect. The measurements executed till now do not provide conclusive evidence of the phenomenon. The measurements of Gordon and of Anwar (see Booij, 1981b) show toomany inconsistencies. E.g., some measurements reveal an appreciable hysteresis of the turbulence energy, and others do not. (Compare Anwar and Atkins (1980 and 1982)).

The various models used in this investigation all yield virtually the same small hysteresis effect. (See fig. 19 for the k-model) This was already expected, (see Booij, 1981a) because of the short reproduction times of k and ε.

An attempt has been made to reproduce measurements of Anwar and Atkins (1980) with the k-model. The variation with time of the surface velocity could approximately be matched by imposing an appropriate pressure gradient see fig. 20a. The smooth bed of the flume was represented by means of a properly varying roughness height. Most aspects of the flow reproduced well, but the hysteresis effect was much smaller than the effect mentioned by Anwar and Atkins (1980) (see fig. 20b).

If more reliable measurements confirm the hysteresis effects, then the models of the eddy viscosity type, as used in this investigation, will have to be adjusted or replaced by more realistic models.

Conclusions

Measurements of steady free surface channel flow yield almost logarithmic velocity profiles. The computations for steady flow in the one-dimensional flow model with the four models used, k-ε-model, k-model, mixing-length model and simple eddy viscosity model, all reproduce these profiles good if they are properly tuned. The k-ε-model and the k-model yield small deviations of the logarithmic profile, but these deviations are smaller than the uncertainty from the measurements. In tidal flow the models give nearly the same almost logarithmic velocity profiles exept for a period around slack water, which is in agreement with most measurements. Around slack water the models give somewhat different profiles. All four models however, are less reliable around slack water. The phase lag of the velocities with respect to the free surface slope reproduces well in all models, but this is not surprising as a depth-averaged model leads already to the same phase lag. No model yields a hysteresis effect of the shear stress with respect to the velocity as mentioned by some investigators.

The agreement of the models is not really surprising as only the viscosity in the lower part of the flow is important for the velocity profile at the small roughness heights used. The variation of the tidal flow is so slow that the rate of change of k and ε may be neglected in their transport equations except around slack water. Larger differences between the different models are only to be expected if these rate of change terms are important, or if the diffusion of k plays an important role.

Considering the agreement of the results of the various models, generally the simple eddy viscosity model should be preferred as the computing time needed is the shortest by far. The usefulness of the k-ε-model is small as it is already unstable for quite small time steps. Choosing the first grid point farther from the bed improves the possible time step, but at a fractional depth of 0.1 still 720 time steps in a tidal cycle are needed. This choice of the first grid point, however, influences the results of the viscosity and therefore of the velocity and the shear stress around slack water. The depth grid has to be chosen with care,

to give the best results. The often used equidistant spacing can give considerable errors.

The physical base of the k-model and especially of the k-ε-model is quite weak. The constants used in the model should actually vary over the depth or over the tidal phase. The calibration of the k-model and especially of the k-ε-model in the situation of the almost steady flow around maxumum velocity can give wrong results around slack water. In the k-ε-model the calibration chosen does not fulfill the required conditions near the bed but gives good overall results.

The boundary conditions at the free surface are poorly known. In this investigation the boundary condition of Hossain is adopted, as the boundary condition most often applied, taking the ε-gradient zero, gives wrong results. The results of the k-ε-model, however, are strongly dependent on the choice of the constants and boundary conditions.

In rivers and estuaries the k-ε-model seems not appropriate because of the short time step needed. If the specification of the length scale is difficult, the k-ε-can be used to determine the behaviour of the length scale and so of the viscosity, but large computations can then be best executed with a simple eddy viscosity model using the eddy viscosity specified in this way.

The computations in this investigation are limited to flows in tidal channels, for which the one dimensional flow model can be used. This model is not appropriate for very high tidal waves (e.g. $|\zeta|/h>0.1$) and near closed ends of tidal channels, where convective derivatives can be important. The computations are executed for tidal flows without a nett discharge over the tidal period at some roughness values and velocities, typical for tidal channels. The conclusions, arrived at, however, are generally valid for flows in tidal channels.

References

Atkins, R., 1980, "Turbulence measurements using a small electragnetic current meter in open channel flows", Hydraulic Research Station Wallingford, Report no. IT 196.

Anwar, H.O., and Atkins, R., 1980, "Turbulence measurements in simulated tidal flow", J. Hydr. Div. ASCE, 106, HY8, pp. 1273-1289.

Anwar, H.O., and Atkins, R., 1982, closure of the discussion to: "Turbulence measurements in simulated tidal flow", J. Hydr. Div. ASCE, 108, HY2, pp. 286-289.

Booij, R., 1981a, "Reproduction of velocity and shear stress profiles in estuaries by some one-dimensional mathematical models (interim report)", Delft Univ. of Techn., Dept. of Civil Engng., Lab. of Fluid Mech., Internal report 2 - 81.

Booij, R., 1981b, discussion to: Anwar H.O. and Atkins R., "Turbulence measurements in simulated tidal flow", J. Hydr. Div. ASCE, 107, HY7, pp. 951-953.

Boussinesq, J., 1877, "Théorie de l'écoulement tourbillant", Mém. Prés. Acad. Sci., 23, p. 46.

Bowden, K.F., et al., 1959, "The distribution of shearing stresses in a tidal current", Geophys. J.R. astr. Soc., 2, pp. 288-305.

Bradshaw, P., et al., 1981, "Engineering Calculation Methods for Turbulent Flow", Academic Press.

Delft Hydraulics Laboratory, 1973, "Computational methods for the vertical distribution of flow in shallow water", report W 152.

Ellison, T.H., 1960, "A note on the velocity profile and longitudinal mixing in a broad open channel", J. Fluid Mech., 8, pp. 33-40.

Gordon, C.M., 1975, "Sediment entrainment and suspension in a turbulent tidal flow", Marine Geology, 18, M57-M64.

Hanjalic, K., and Launder, B.E., 1972, "Fully developed asymmetric flow in a plane channel", J. Fluid Mech., 52, p. 301.

Hinze, O., 1959, "Turbulence", McGraw-Hill.

Hossain, M.S., 1980, "Mathematische Modellierung von turbulenten Auftriebsströmungen", Thesis, Universität Karlsruhe.

Johns, B., (App. Odd, N.), 1966, "On the vertical structure of tidal flow in river estuaries", Geophys. J.R. astr. Soc., 12, pp. 103-110.

Johns, B., 1978, "The modeling of tidal flow in a channel using a turbulence energy closure scheme", J. Phys. Oceanogr., 8, pp. 1042-1049.

Karman, Th. Von, 1930, "Mechanische Ähnlichkeit und Turbulenz", Nachr. Ges. Wiss. Göttingen, Math. Phys., K1, p. 58.

Kolmogorov, A.N., 1942, "Equations of turbulent motion in an incompressible turbulent fluid", Izv. Akad. Nauk. SSSR, Ser. Fiz., VI, no.1-2, pp. 56-58.

Knight, D.W., 1975, "Velocity and shear stress distributions in oscillatory flow", Proc. 16th. Congress IAHR, Sao Paulo, 1, pp. 66-72.

Launder, B.E., and Spalding, D.B., 1972, "Mathematical models of Turbulence", Academic Press.

Nakagawa, H., et al., 1975, "Turbulence of open channel flow over smooth and rough beds", Proc. of the Japan Soc. of Civil Engns, No 241, pp. 155-168.

Prandtl, L., 1925, "Bericht über Untersuch zur ausgebildeten Turbulenz", Z. angew. Math. Mech., 5, p. 136.

Prandtl , L., 1945, "Über ein neues Formelsystem für die ausgebildeten Turbulenz", Nachr. Akad. Wiss. Göttingen, Math. Phys. Klasse, p. 6.

Proudman, J., 1953, "Dynamical Oceanography", Methuen.

Rodi, W., 1980, "Turbulence models and their application in hydraulics", IAHR.

Smith, T.J., and Dyer, K.R., 1979, "Mathematical modelling of circulation and mixing in estuaries", from "Mathematical Modelling of Turbulent Diffusion in the Environment", ed. C.J. Harris, Academic Press, pp. 301-341.

Smith, T.J., and Takhar, H.S., 1977, "The calculation of oscillatory flow in open channels using mean turbulence energy models", University of Manchester, Simon Engineering Laboratories, Report HHS/77/01.

Smith, T.J., and Takhar, H.S., 1979, "On the calculation of the width averaged flow due to long waves in an open channel", J. Hydr. Res., 17, pp. 329-340.

Sternberg, R.W., 1968, "Friction factors in tidal channels with differing bed roughness", Marine Geol.,6, pp. 243-260.

Townsend, A.A., 1976, "The structure of Turbulent Shear Flow", Cambridge Univ. Press, (2nd ed).

Notation

		page
C	resistance coefficient of Chézy	11
C_1	constant in the k-model and k-ε-model	20
C_ν, C_D	constants in the k-model	17/18
$C_{p\varepsilon}, C_{d\varepsilon}$	constants in the k-ε-model	20
$C_{b\varepsilon}$	constant in the free surface boundary condition of ε	24
D_t	turbulence diffusion coefficient	17
g	acceleration due to gravity	8
h	mean free surface level	8
k	kinematic turbulence kinetic energy	17
l_m	mixing-length	16
L	length-scale in the k-model and in the k-ε-model	17
L_t	length-scale in the viscosity	15
N	number of time steps in a tidal cycle	37
Ox, Oz	coordinate axes	8
p	kinematic pressure	18
R	constant appearing in the normalized rate of change terms	11
s	pressure gradient connected with a surface slope	8
S	amplitude of s	10
t	time	8
Δt	time step	36
T_p	tidal period	10
T_k	reproduction time of k	38
T_ε	reproduction time of ε	38
u	longitudinal velocity	8
u_*	friction velocity	10
u_{*_s}	friction velocity in steady flow	10
u_{av}	depth-averaged velocity	11
$u_{av,s}$	depth-averaged velocity in steady flow	11
u_i'	component of the turbulent velocity (i=1,2,3)	17
V_t	velocity scale in the viscosity	15
w	vertical velocity	8
x	longitudinal coordinate	8
x_j	j-th coordinate (j=1,2,3)	18
z	height above the bed	8
z^*	non-dimensional height used for the law of the wall	22
z_0	characteristic roughness height	12

β	ratio of u_{av} and u_*	40
ε	dissipation rate of turbulence energy	19
ζ	displacement of the surface level	8
κ	Von Karman's constant	12
Λ	Lagrangian integral length scale	17
ν	kinematic viscosity	18
ν_t	kinematic eddy viscosity	9
σ_k	constant in the k-model	18
σ_ε.	constant in the ε-model	20
τ	kinematic Reynolds shear stress	8
τ_0	bed shear stress	10
τ_{0s}	bed shear stress in steady flow	10
ω	tidal wave frequency	10
+ (suffix)	normalized	10
' (suffix)	turbulent component	17
max(suffix)	the maximum value over the tidal period	34
min(suffix)	the minimum value over the tidal period and over the depth	38

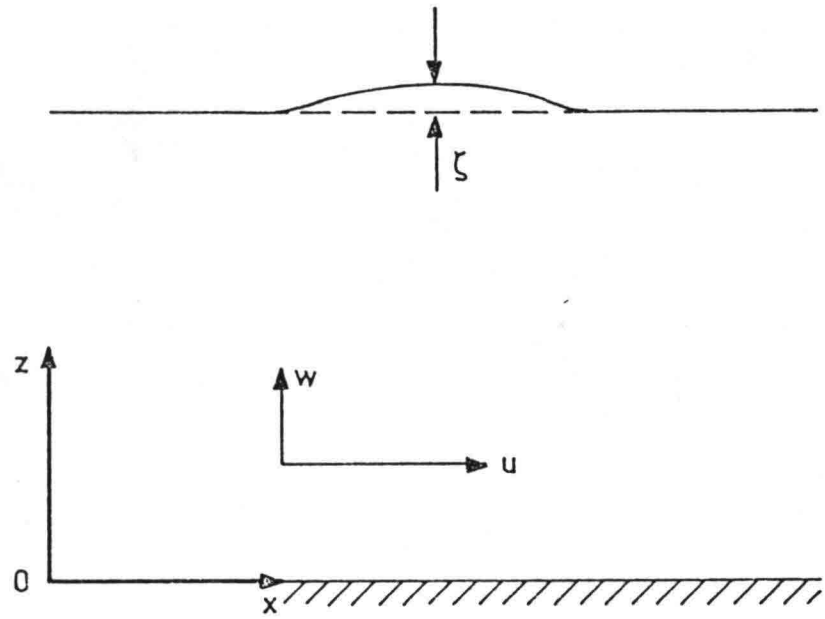

fig. 1. Definition sketch.

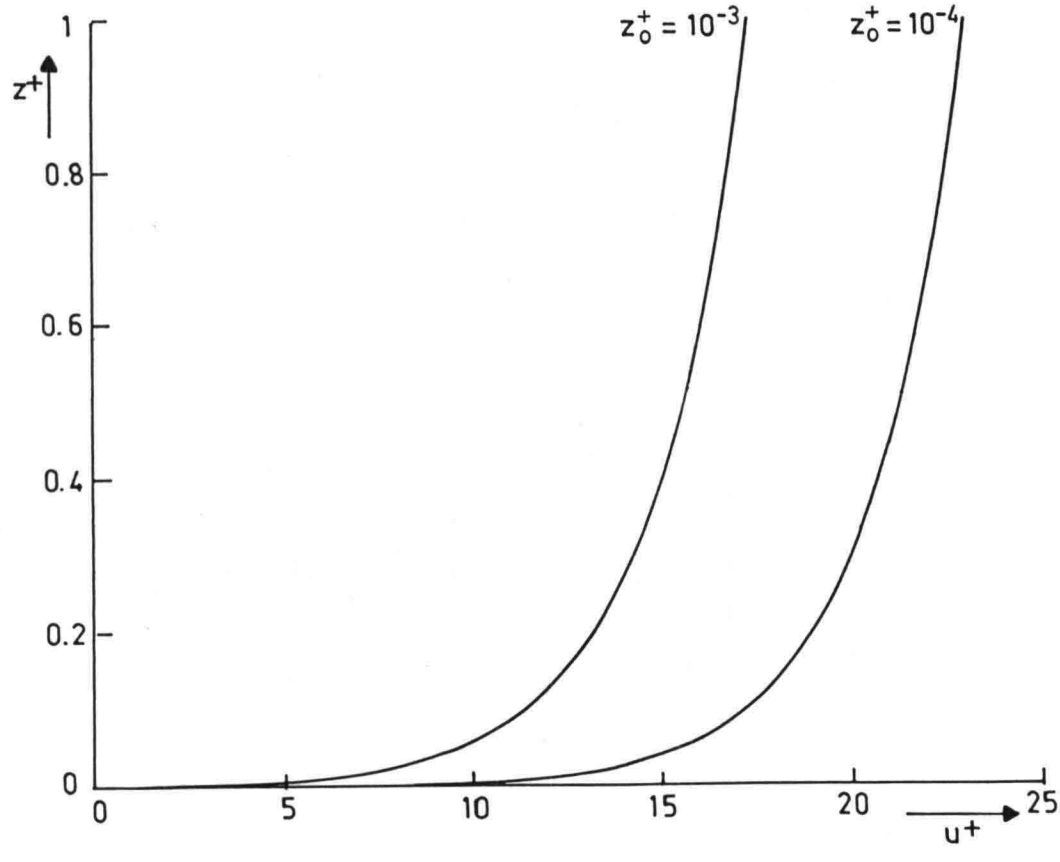

fig. 2. Logarithmic velocity profiles.

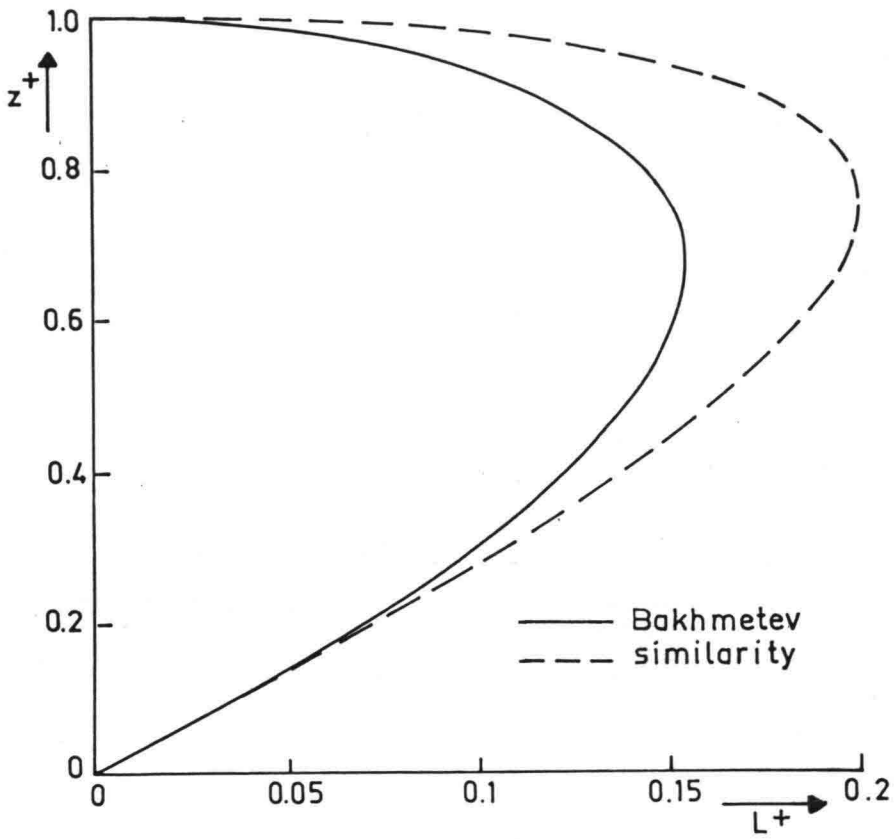

fig. 3. Mixing-length distributions.

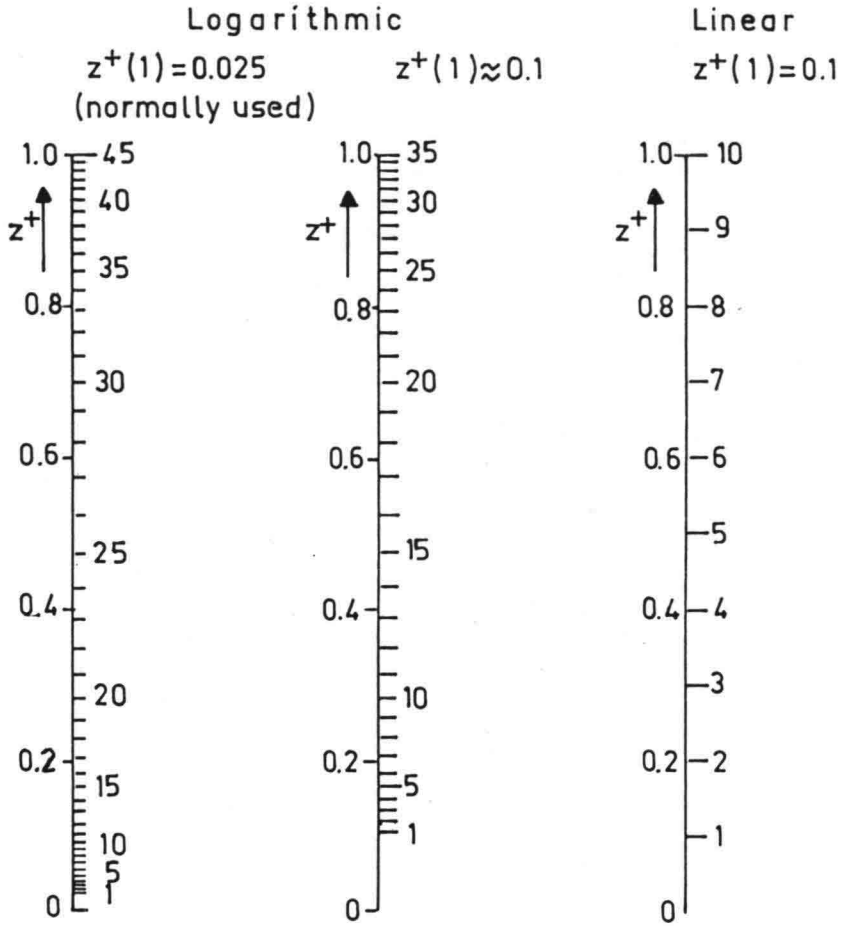

fig. 4. Used space-grids.

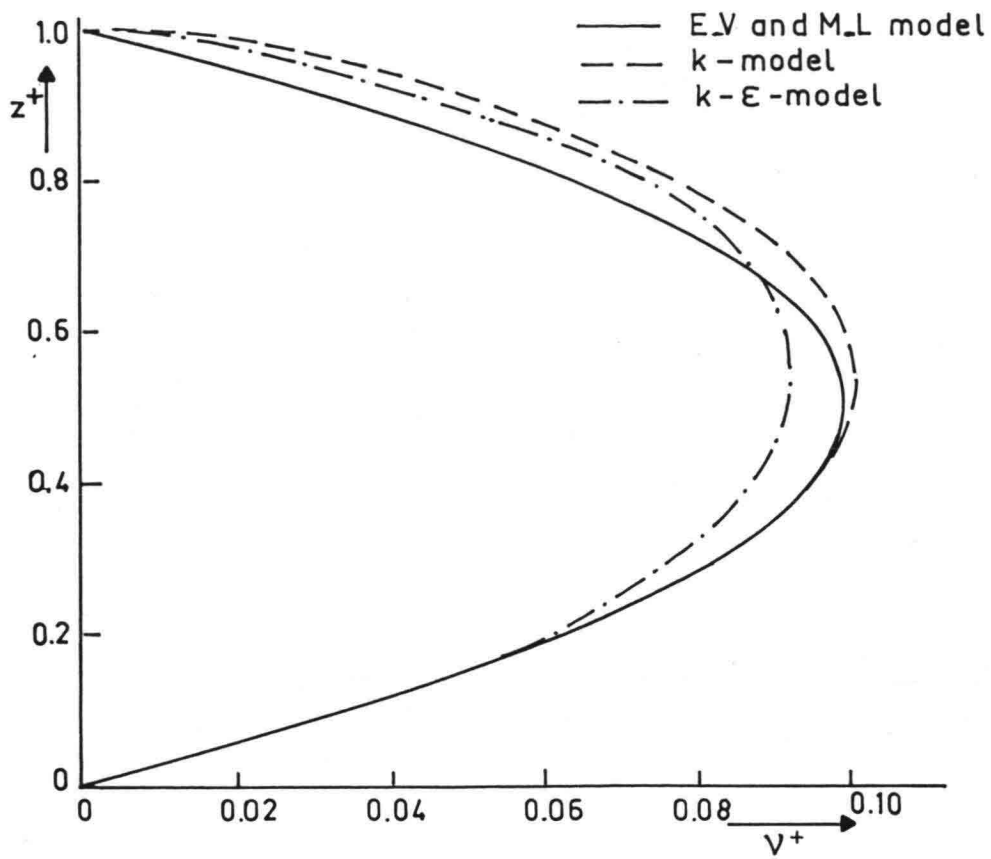

a. Eddy viscosity distributions.

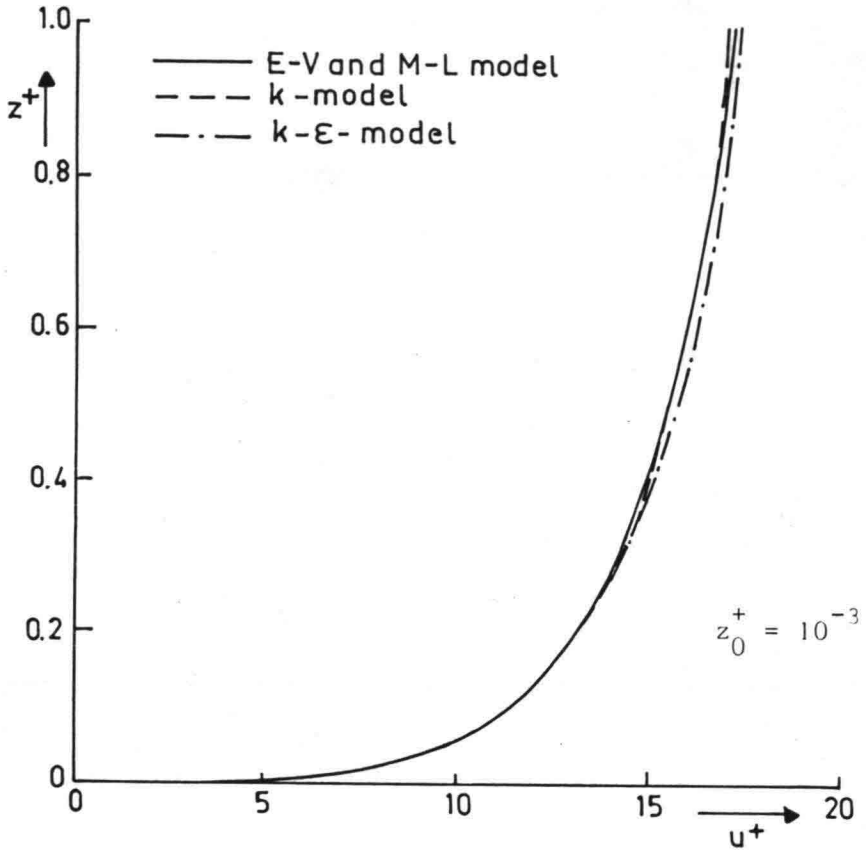

b. Velocity profiles.

fig. 5. Comparison of the results of the various models for steady flow.

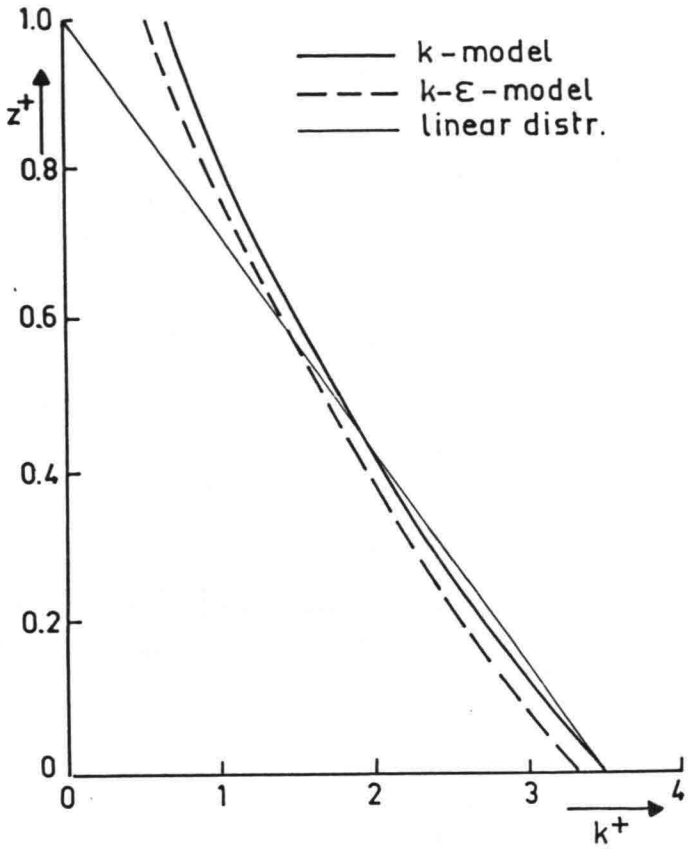

fig. 6. Turbulence energy distributions for steady flow.

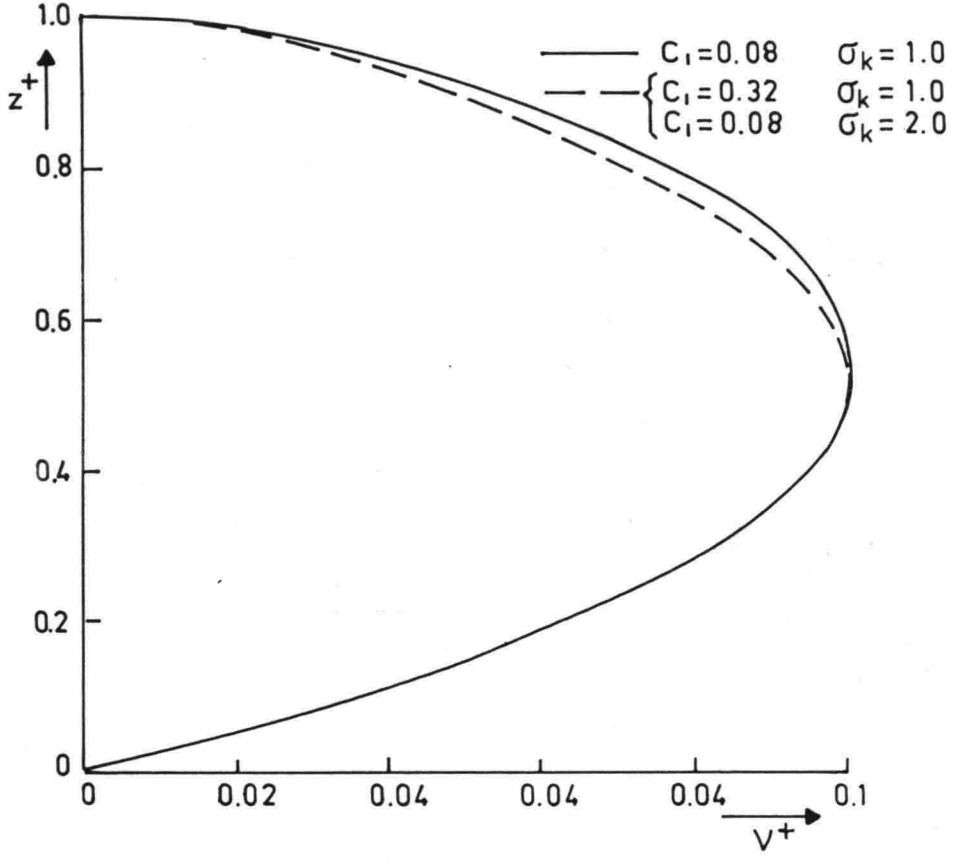

fig. 7. Eddy viscosity distributions for steady flow calculated with the k-model using different constants.

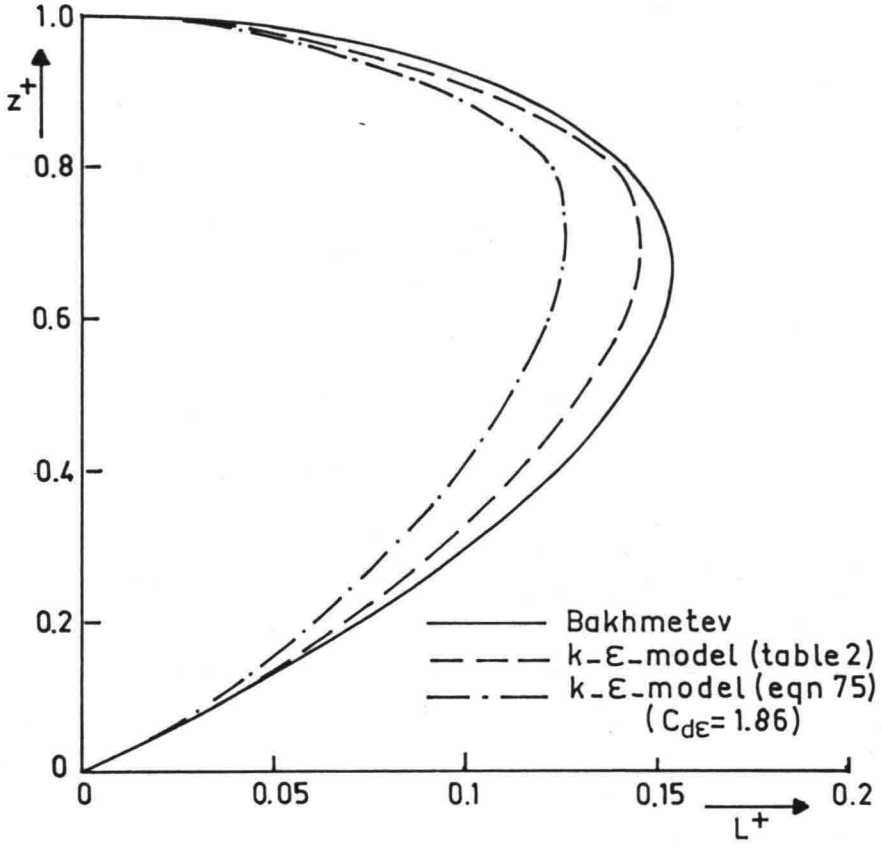

a. Satisfying equation (75).

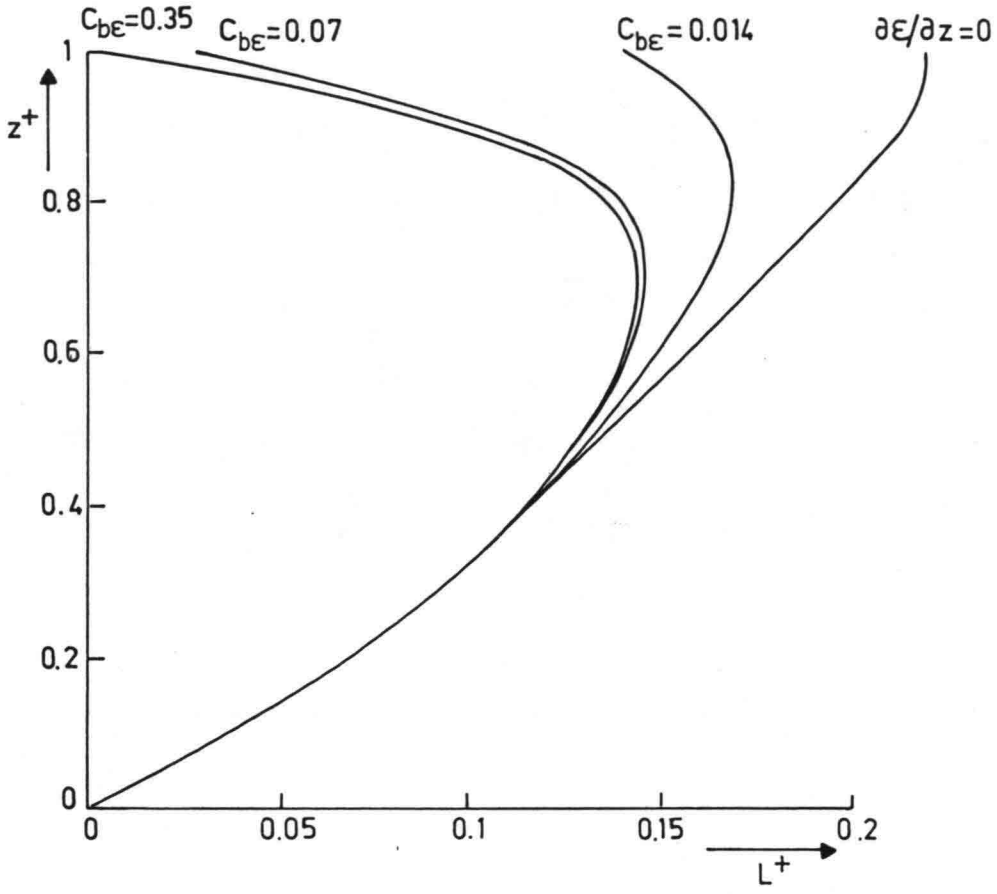

b. Dependence on the free boundary condition for ε.

fig. 8. Length scale distribution calculated with the k-ε-model for steady flow.

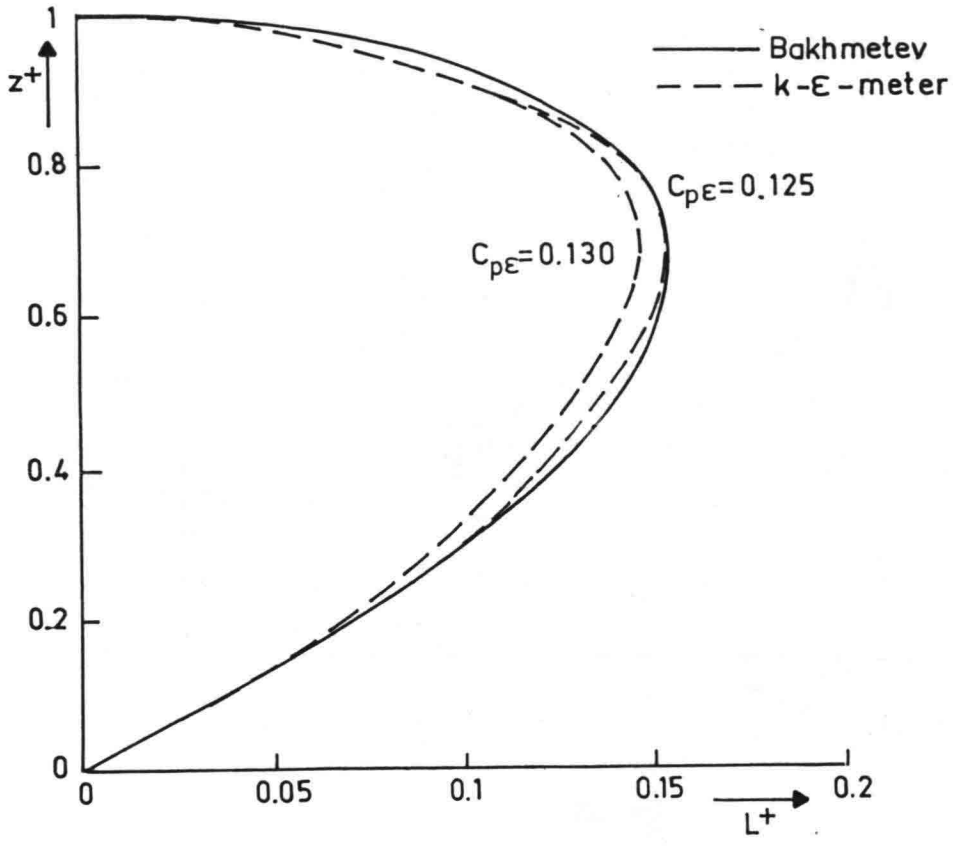

c. Tuning of the k-ε-model for steady flow.

fig. 8. Length scale distribution calculated with the k-ε-model for steady flow.

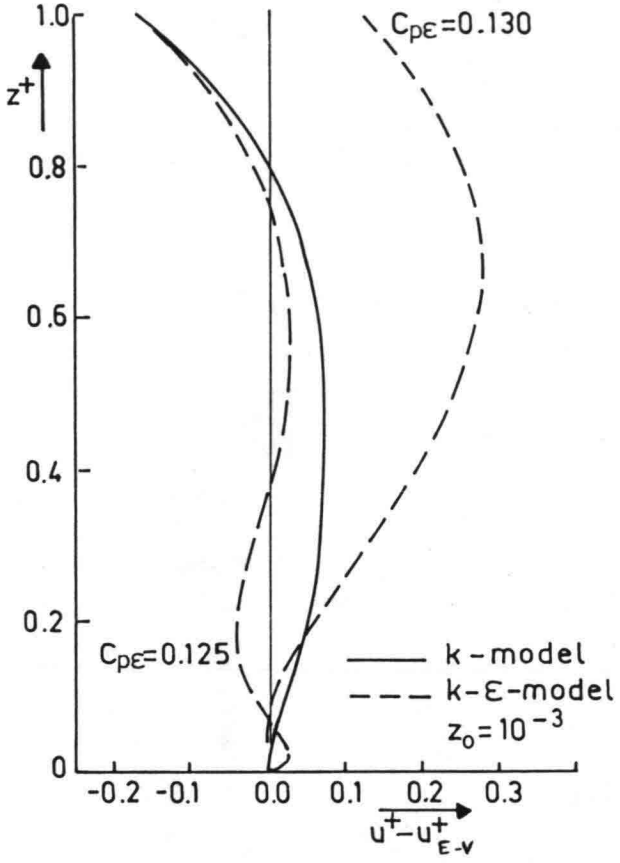

fig. 9. Difference between the velocities calculated with the k-model or k-ε-model and the logarithmic velocity profile of the simple eddy viscosity model.

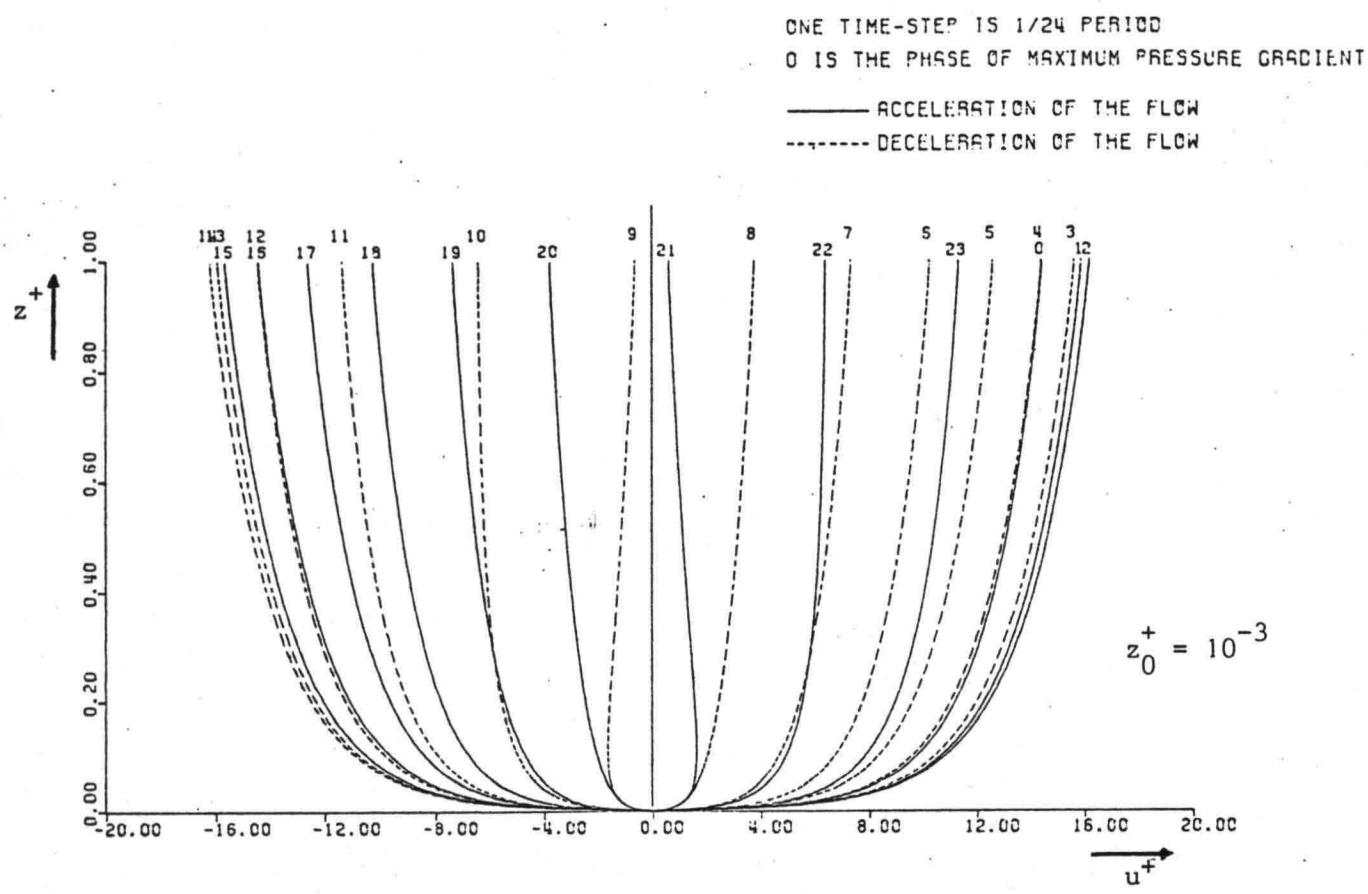

a. Simple eddy viscosity model.

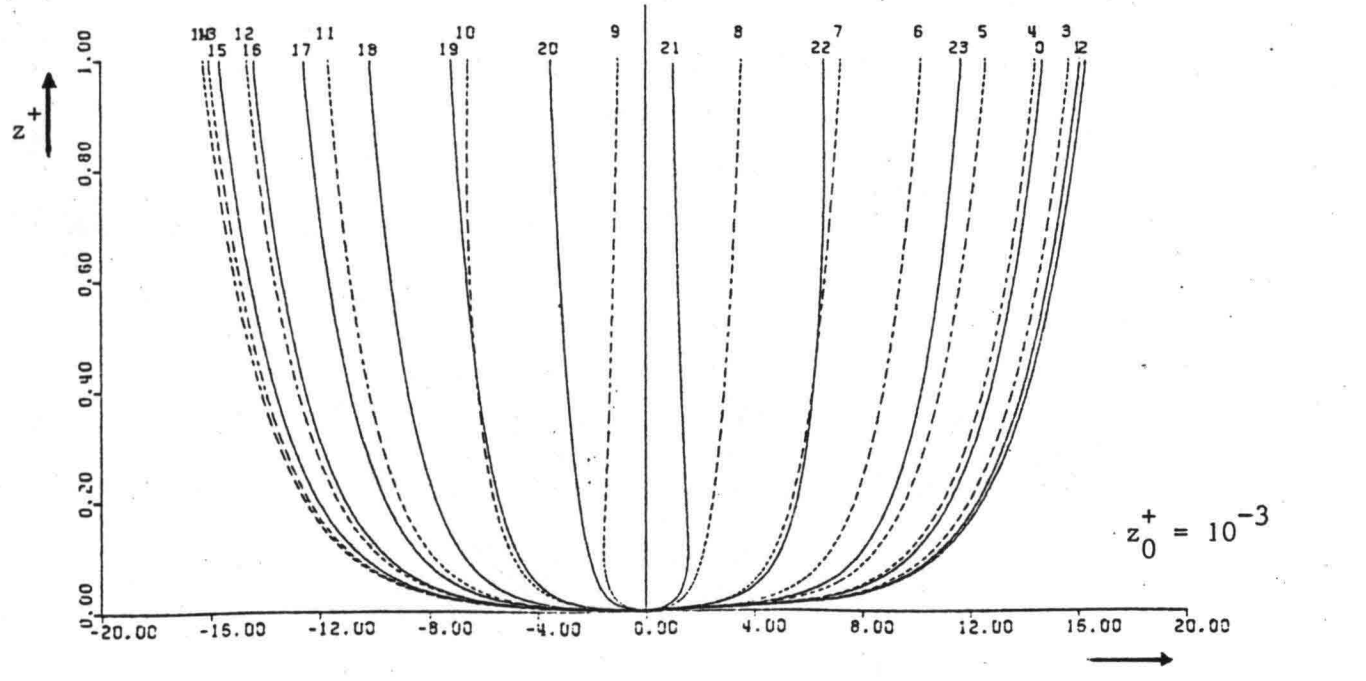

b. Mixing-length model.

fig. 10. Velocity profiles in tidal flow

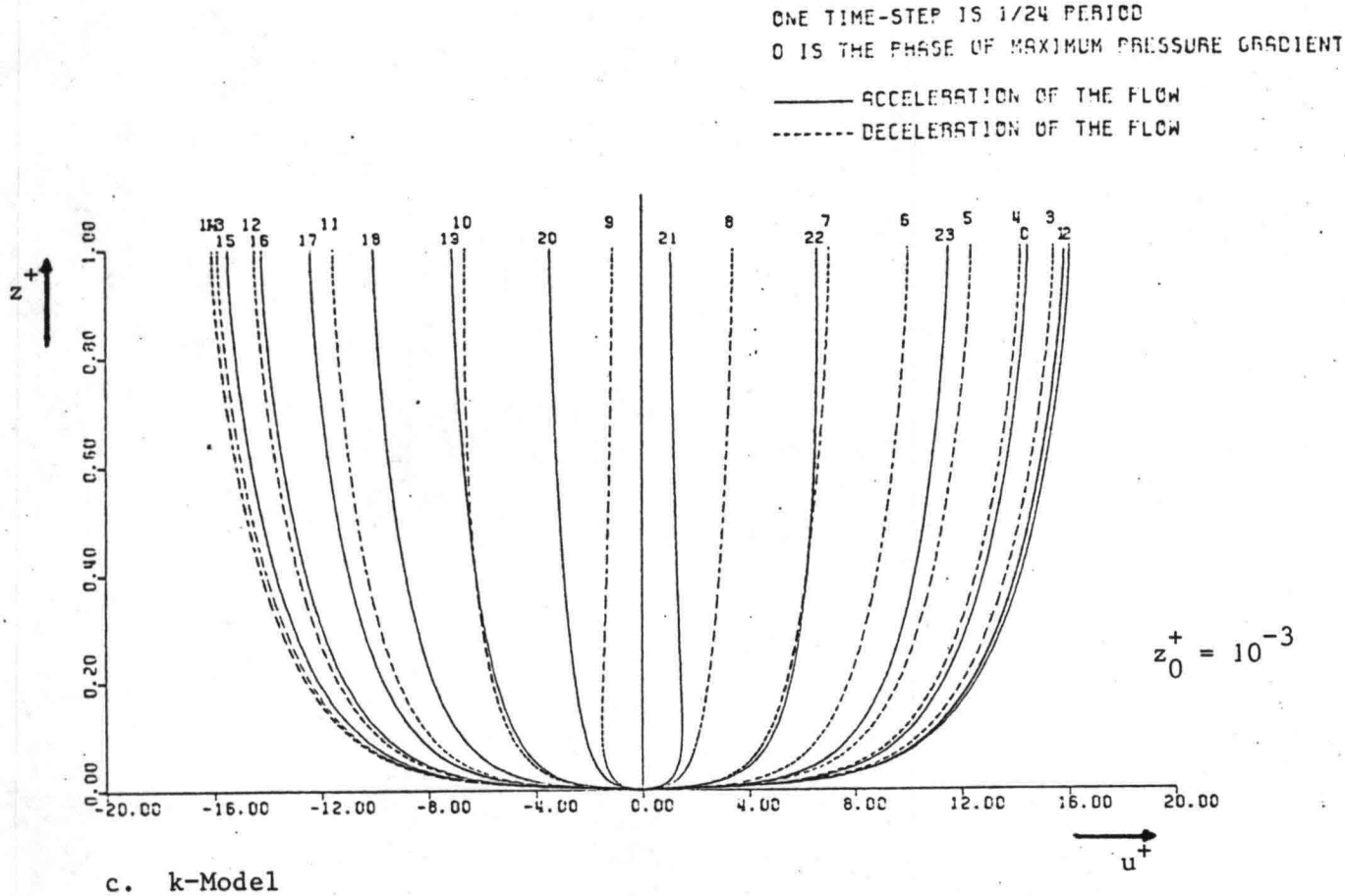

c. k-Model

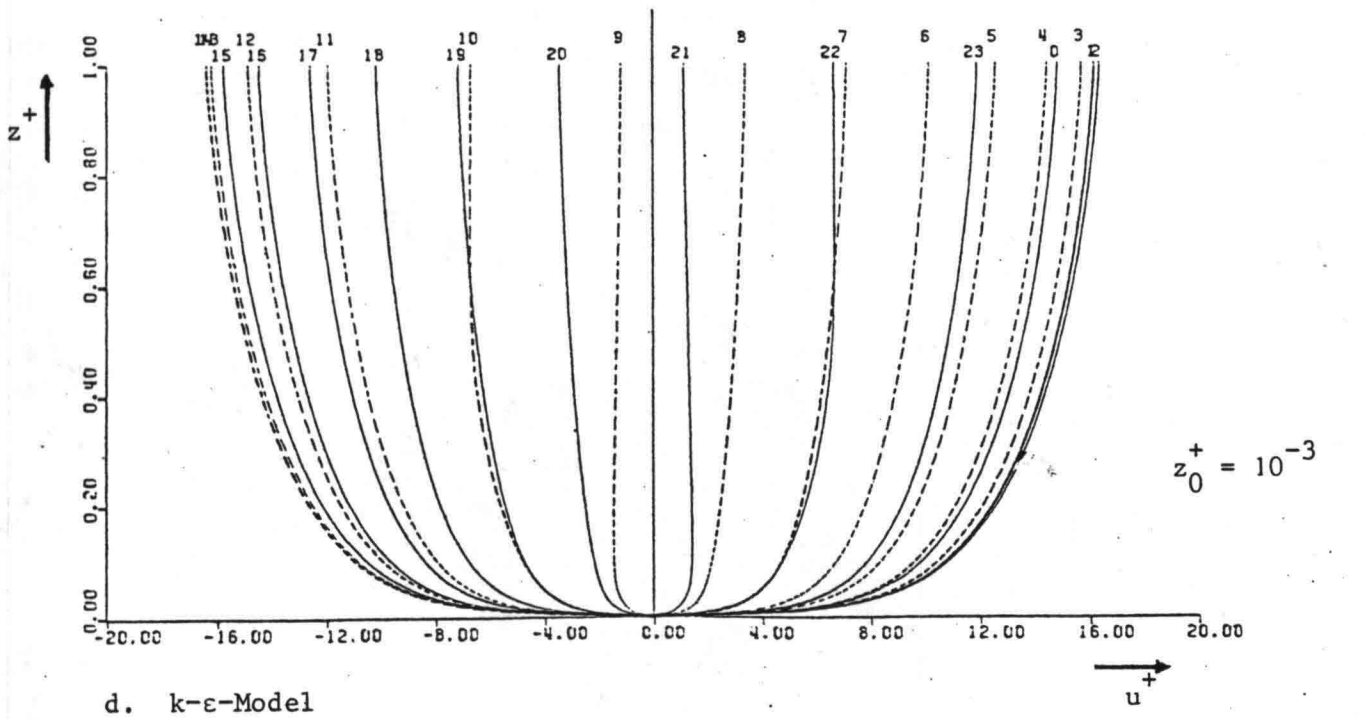

d. k-ε-Model

fig. 10. Velocity profiles in tidal flow

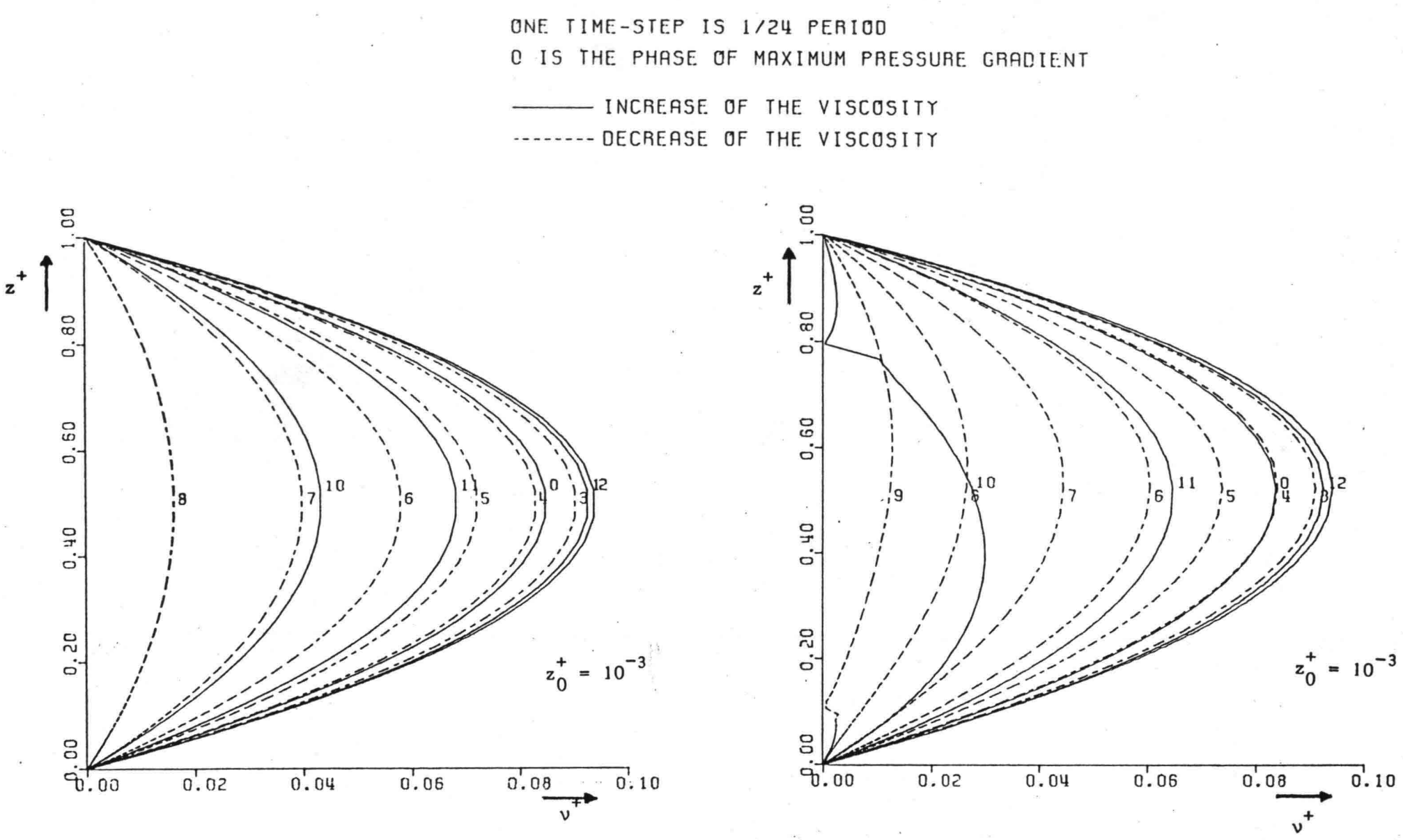

a. Simple eddy viscosity model.

b. Mixing-length model.

fig. 11. Eddy viscosity distributions in tidal flow.

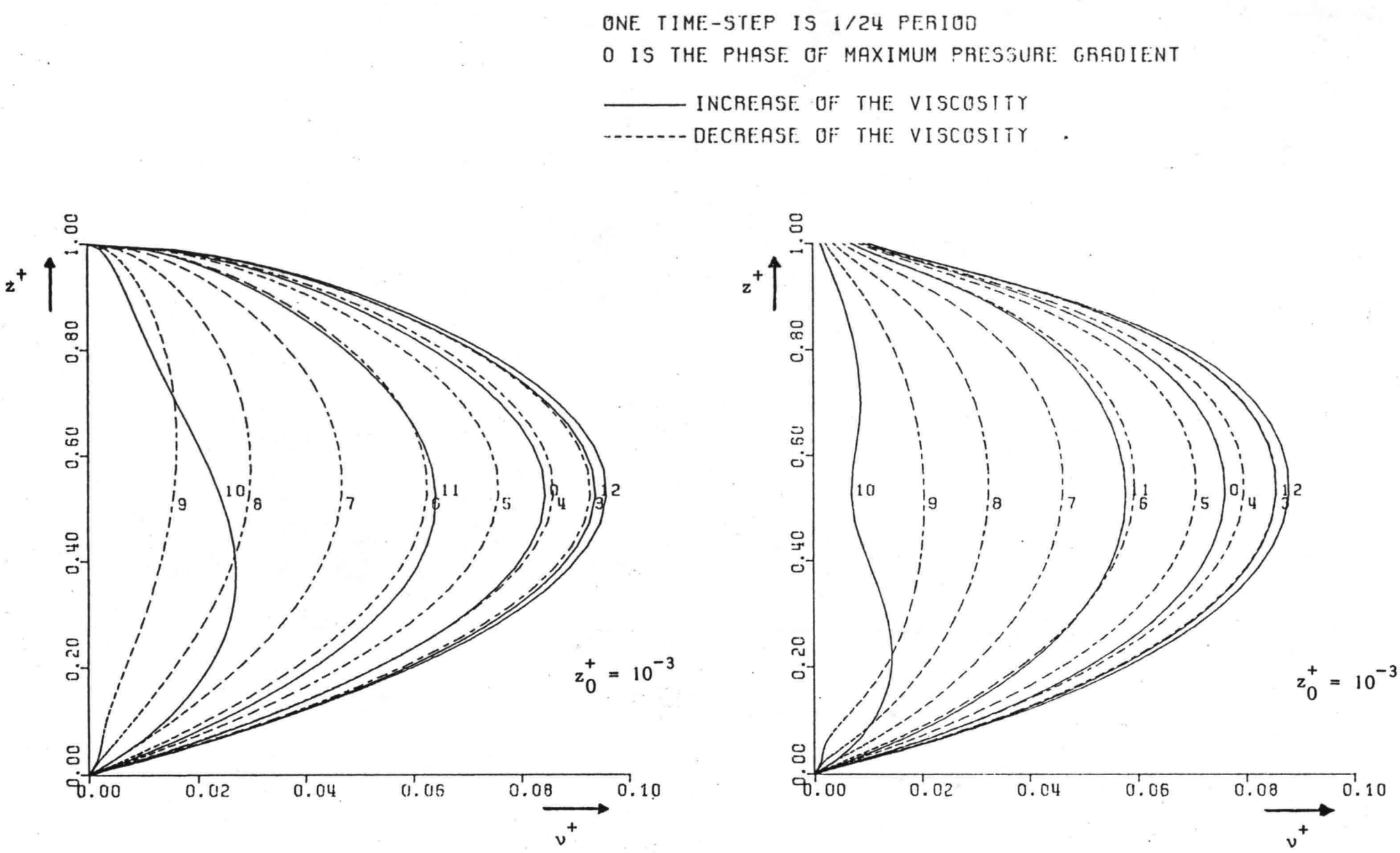

c. k-Model

d. k-ε-Model

fig. 11. Eddy viscosity distributions in tidal flow

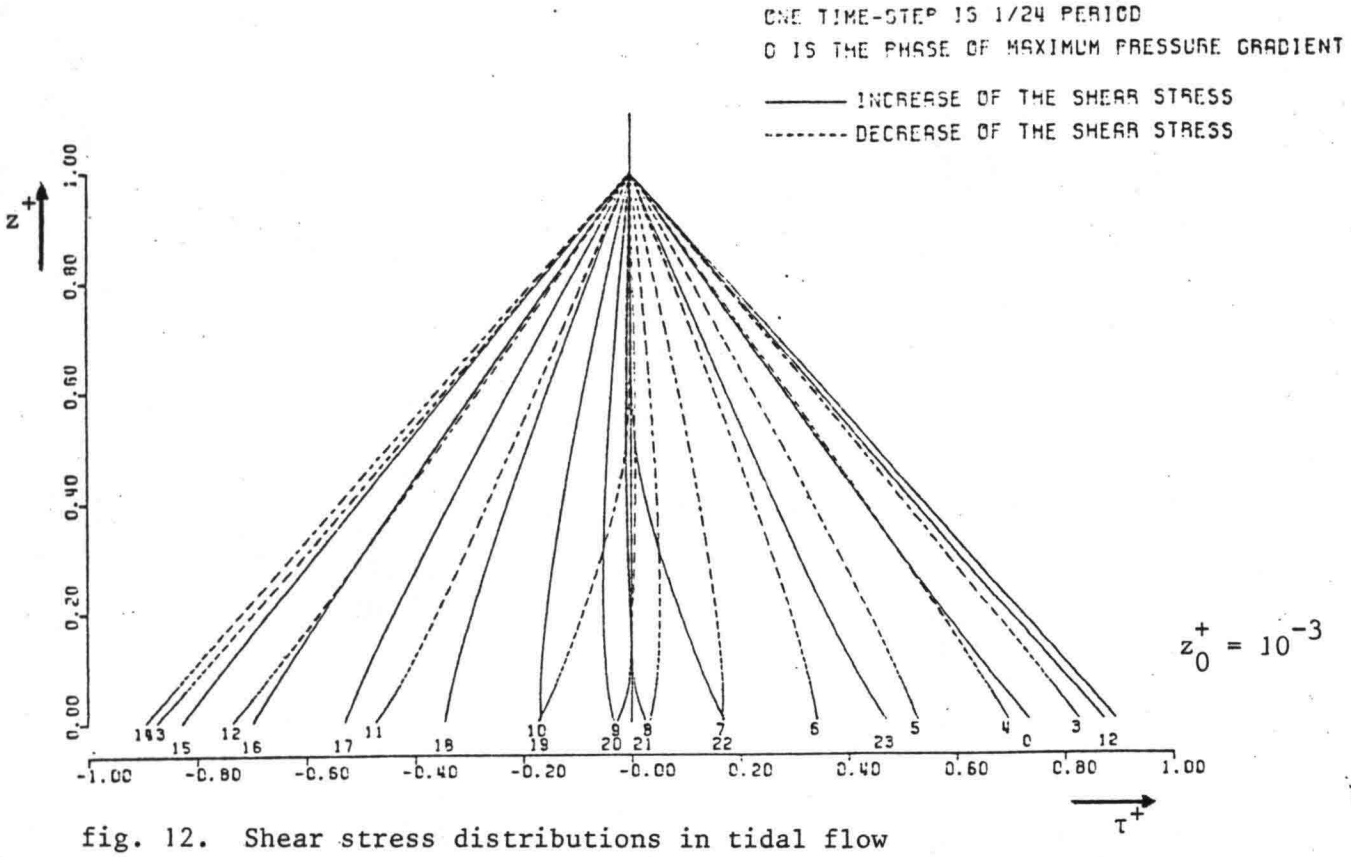

fig. 12. Shear stress distributions in tidal flow predicted with the k-ε-model.

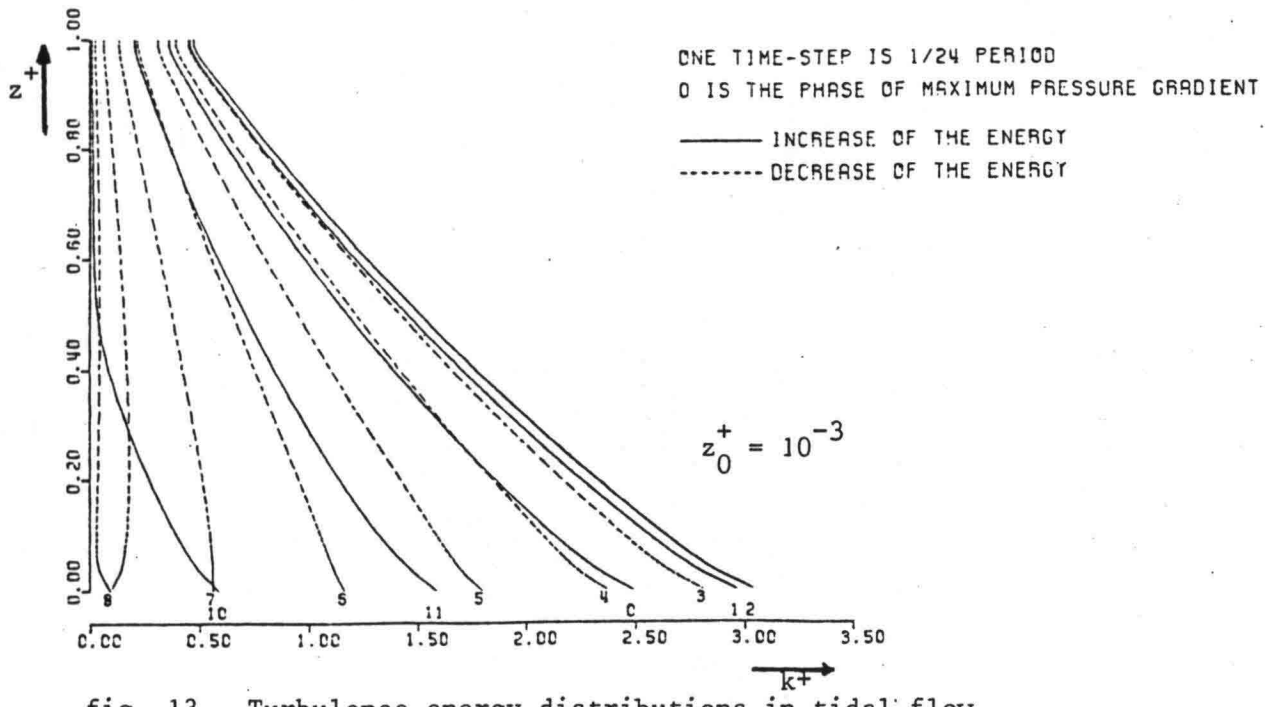

fig. 13. Turbulence energy distributions in tidal flow predicted with the k-ε-model.

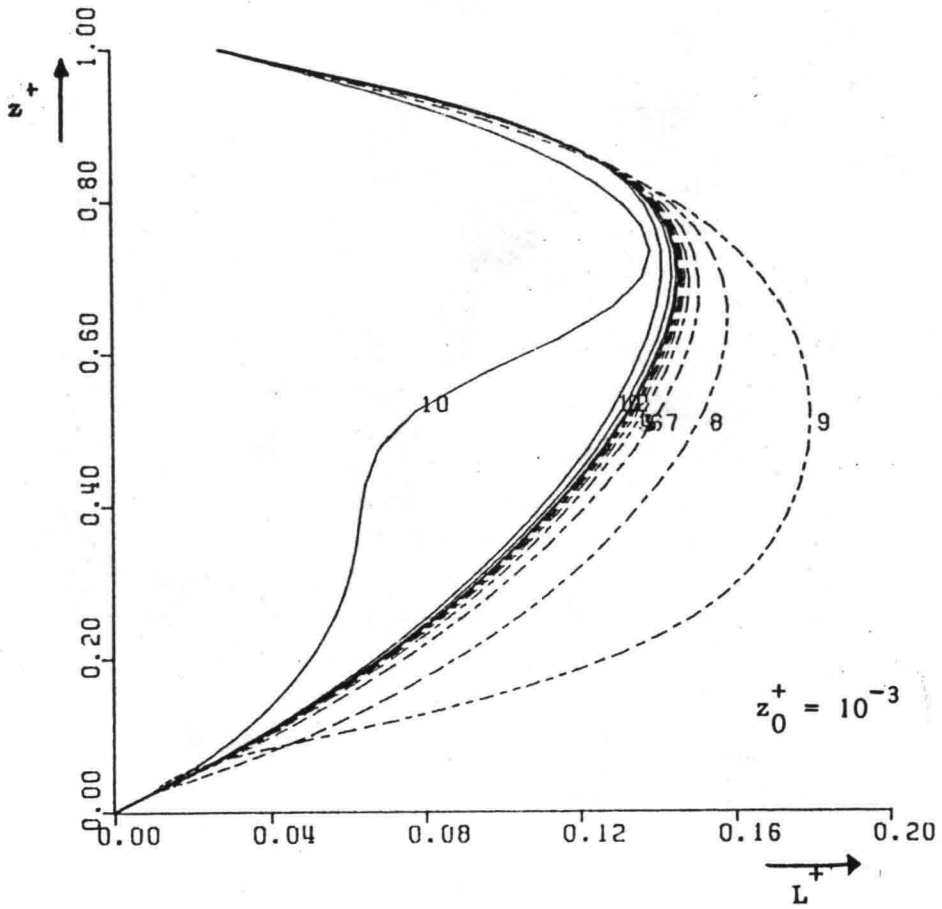

fig. 14. Length scale distributions in tidal flow predicted with the k-ε-model.

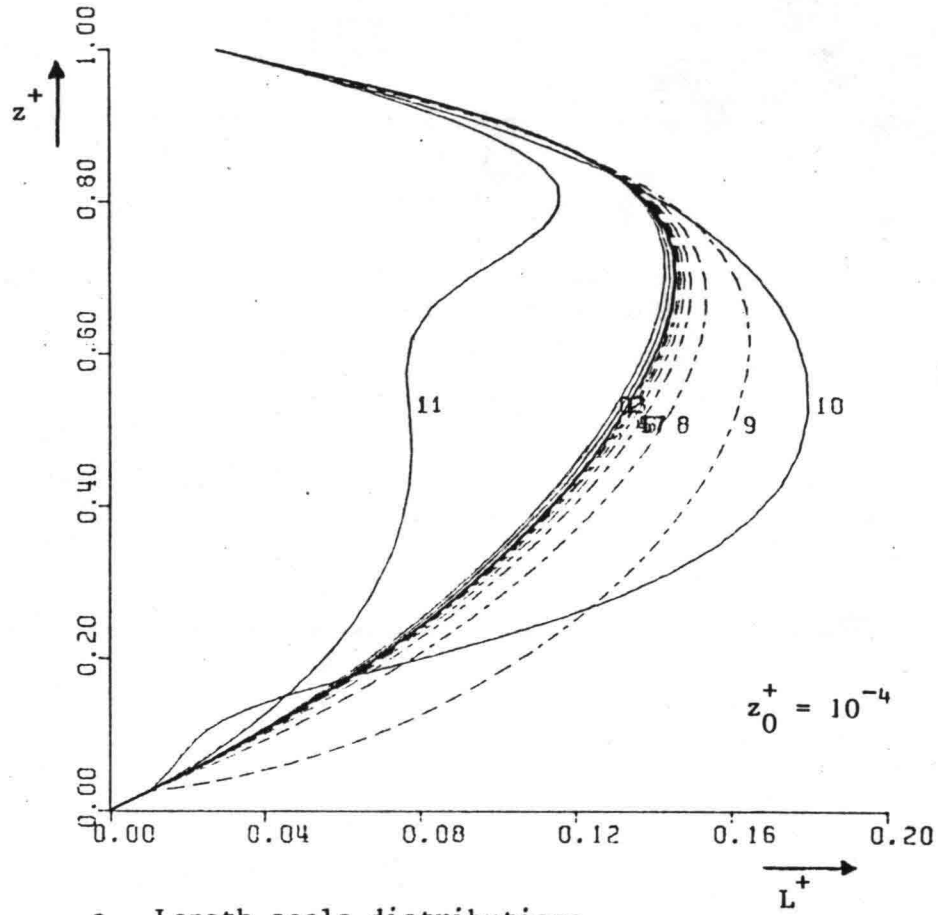

a. Length scale distributions

fig. 15. Predictions with the k-ε-model in tidal flow for a different bed roughness.

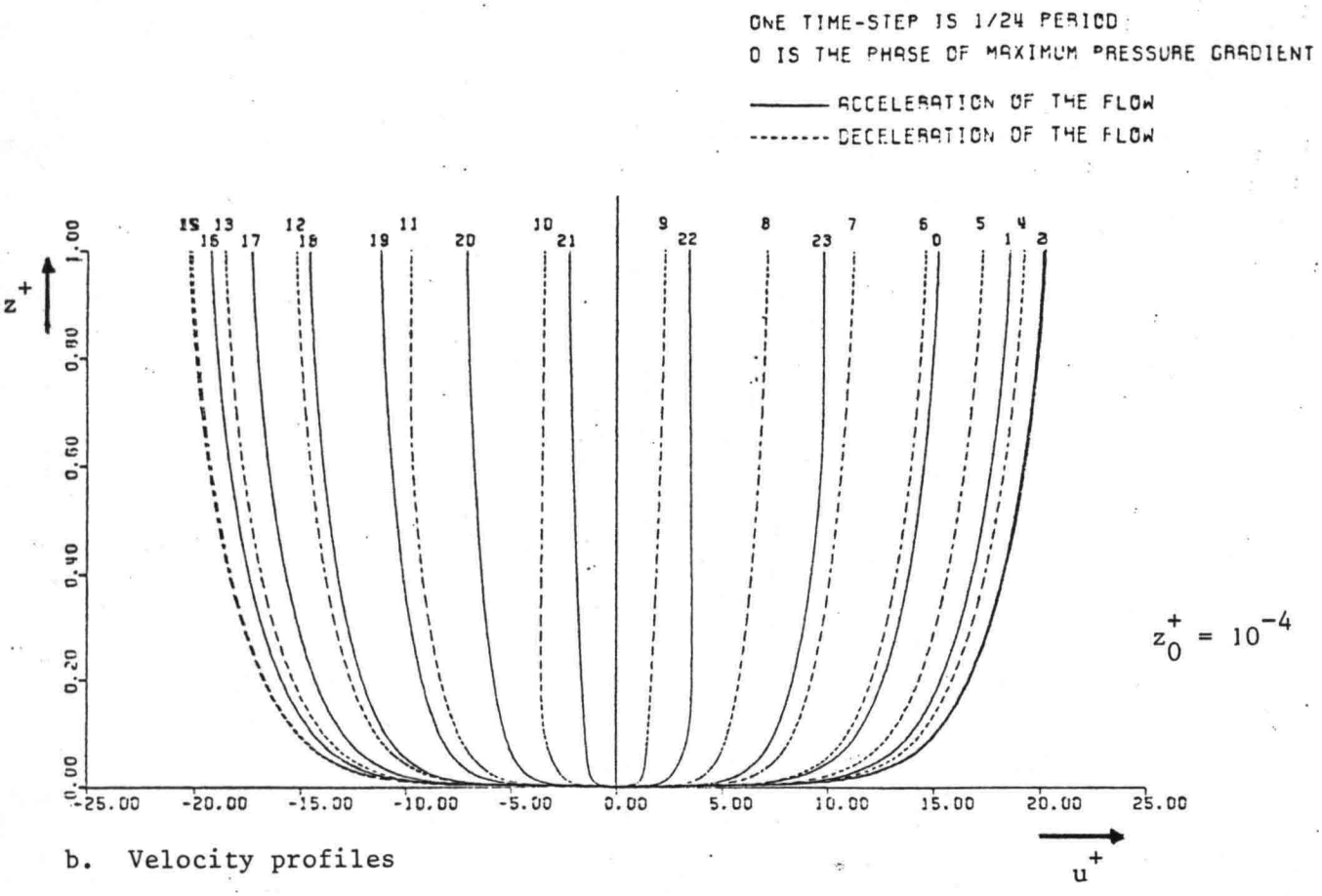

b. Velocity profiles

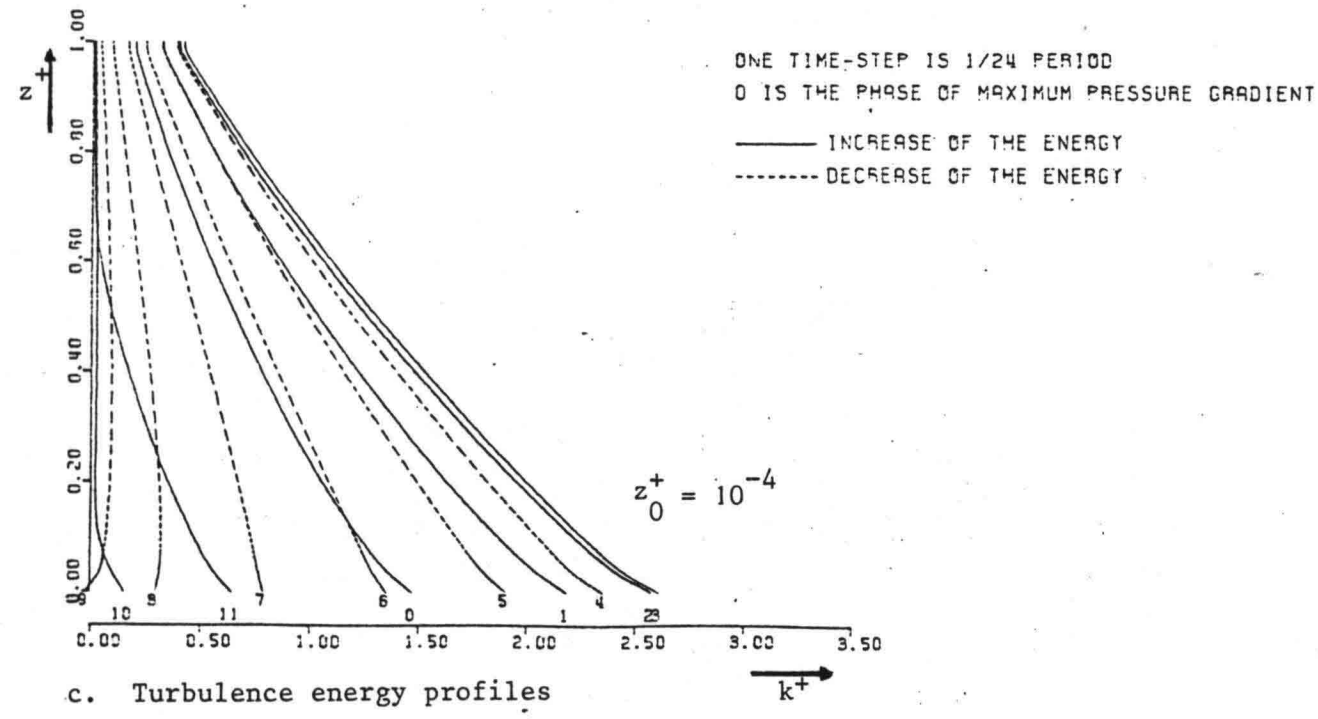

c. Turbulence energy profiles

fig. 15. Predictions with the k-ε-model in tidal flow for a different bed roughness.

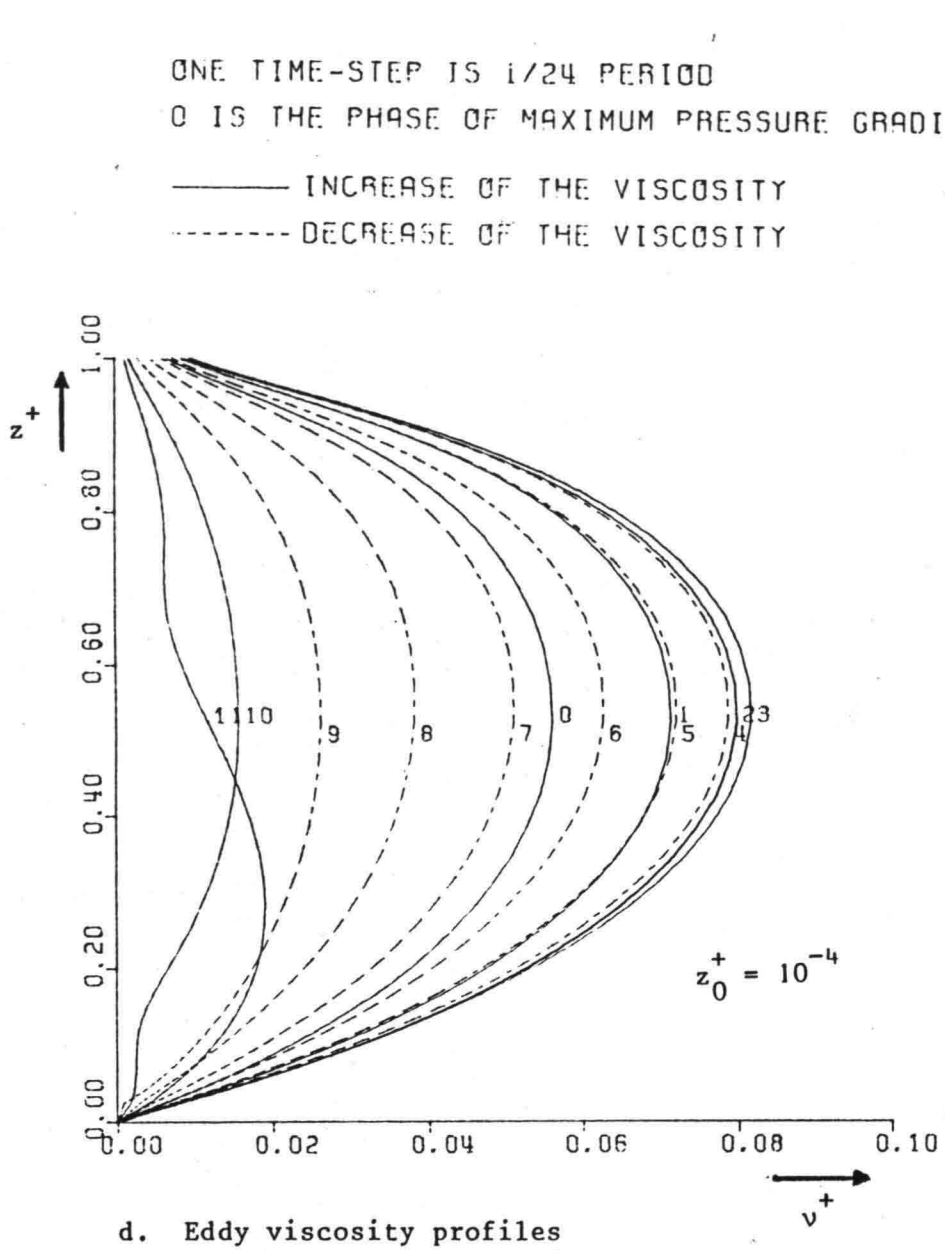

d. Eddy viscosity profiles

fig. 15. Predictions with the k-ε-model in tidal flow for a different bed roughness.

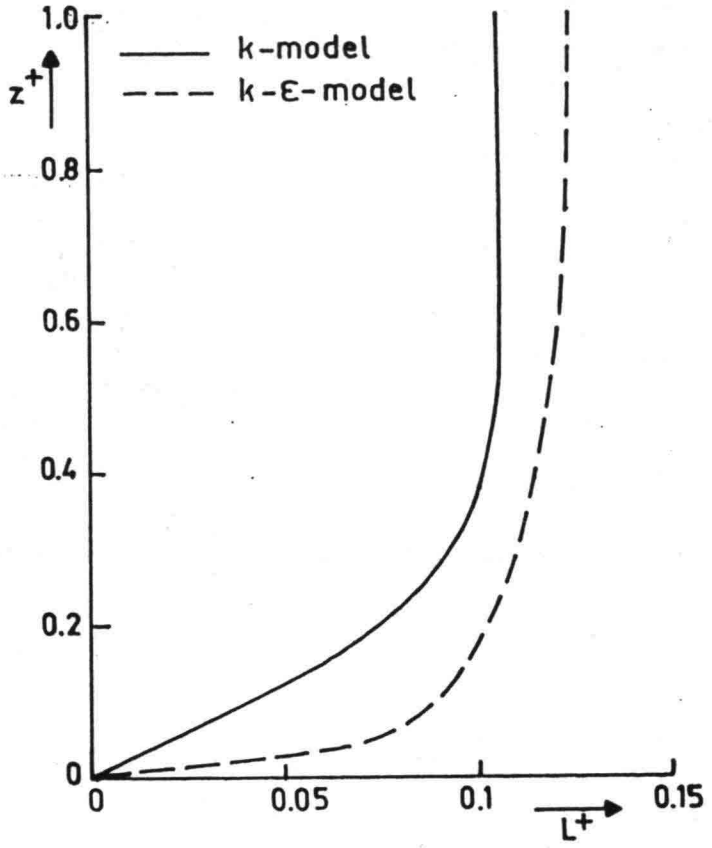

fig. 16. Length scale distributions mentioned by Smith and Takhar (1979).

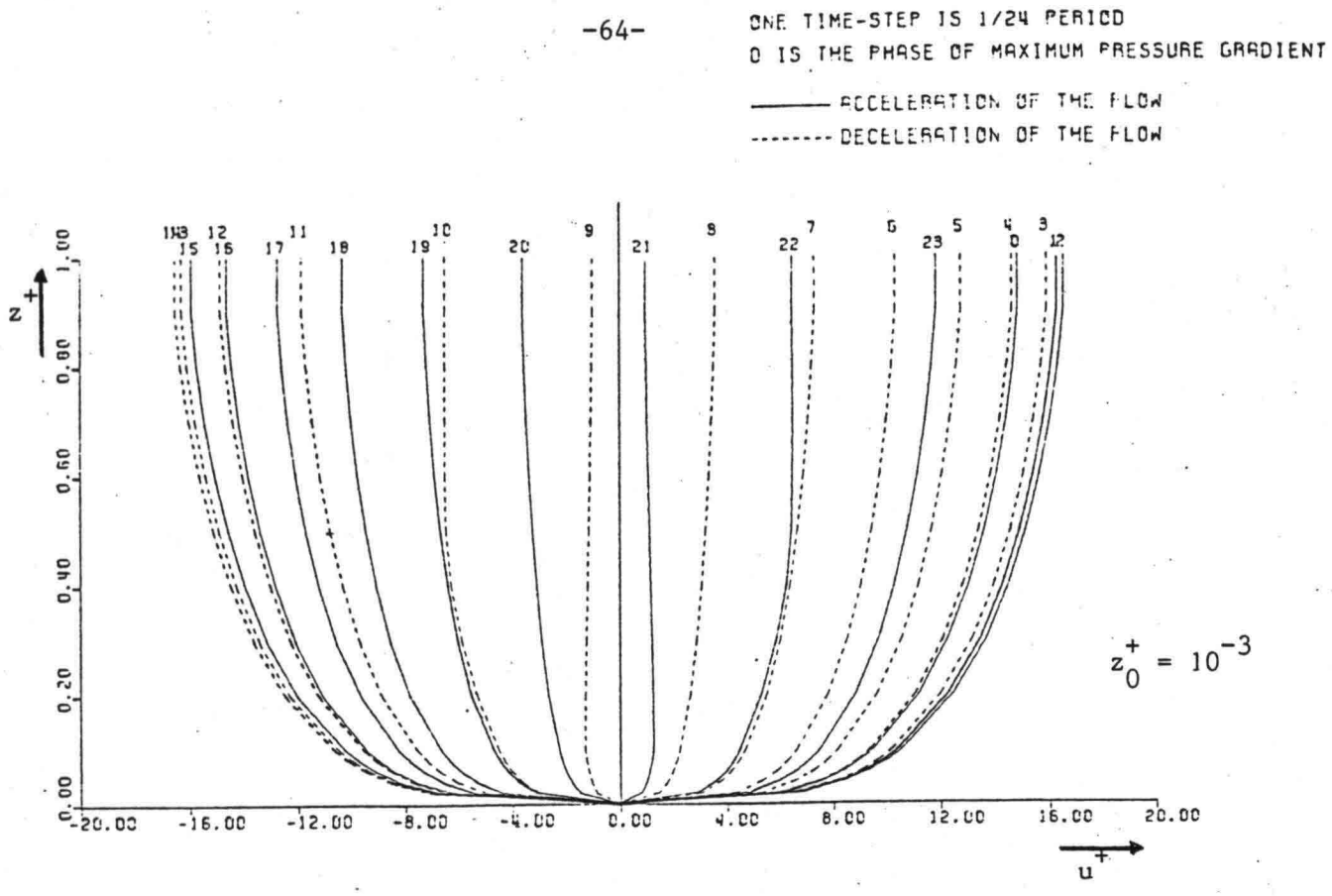

fig. 17. Velocity profiles in tidal flow predicted with the k-ε-model using a coarse equidistant space grid

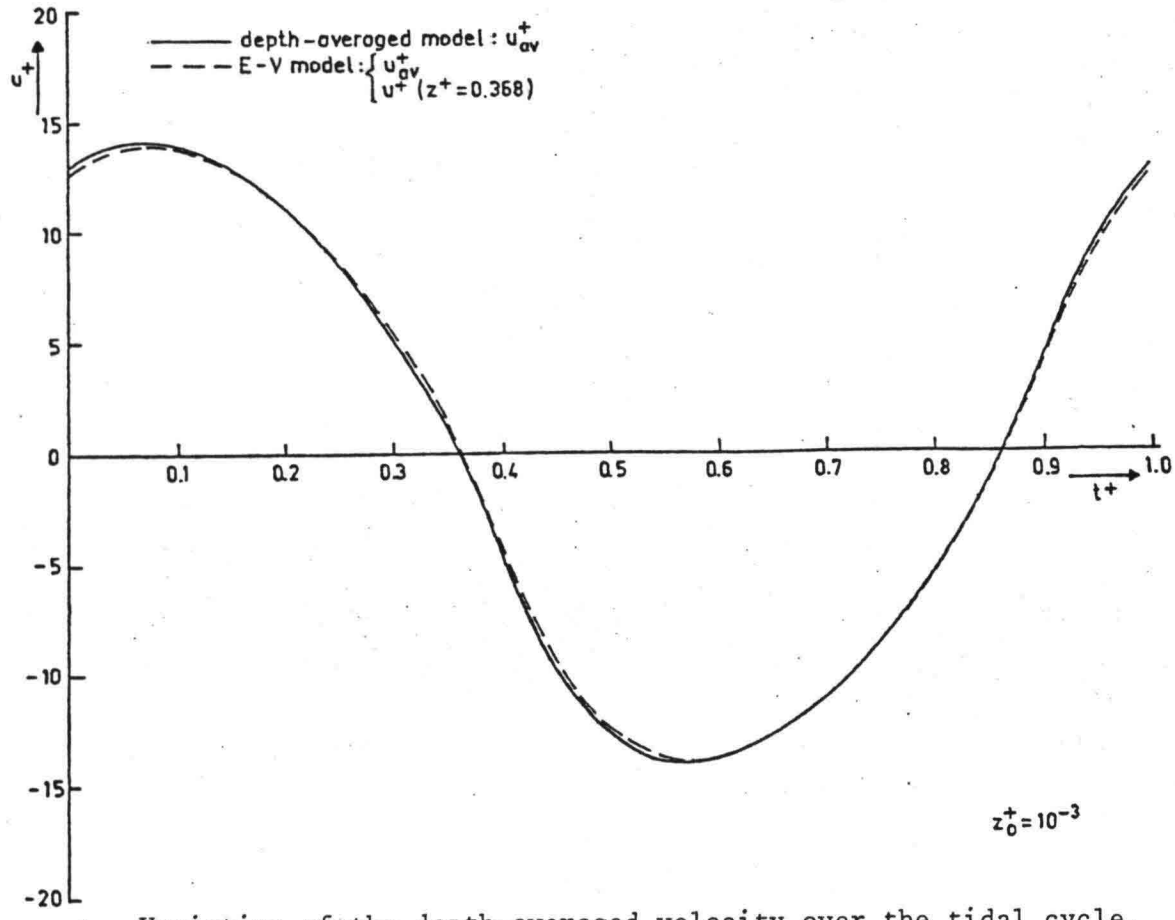

a. Variation of the depth-averaged velocity over the tidal cycle.

fig. 18. Comparison of the simple eddy viscosity model and a depth-averaged model

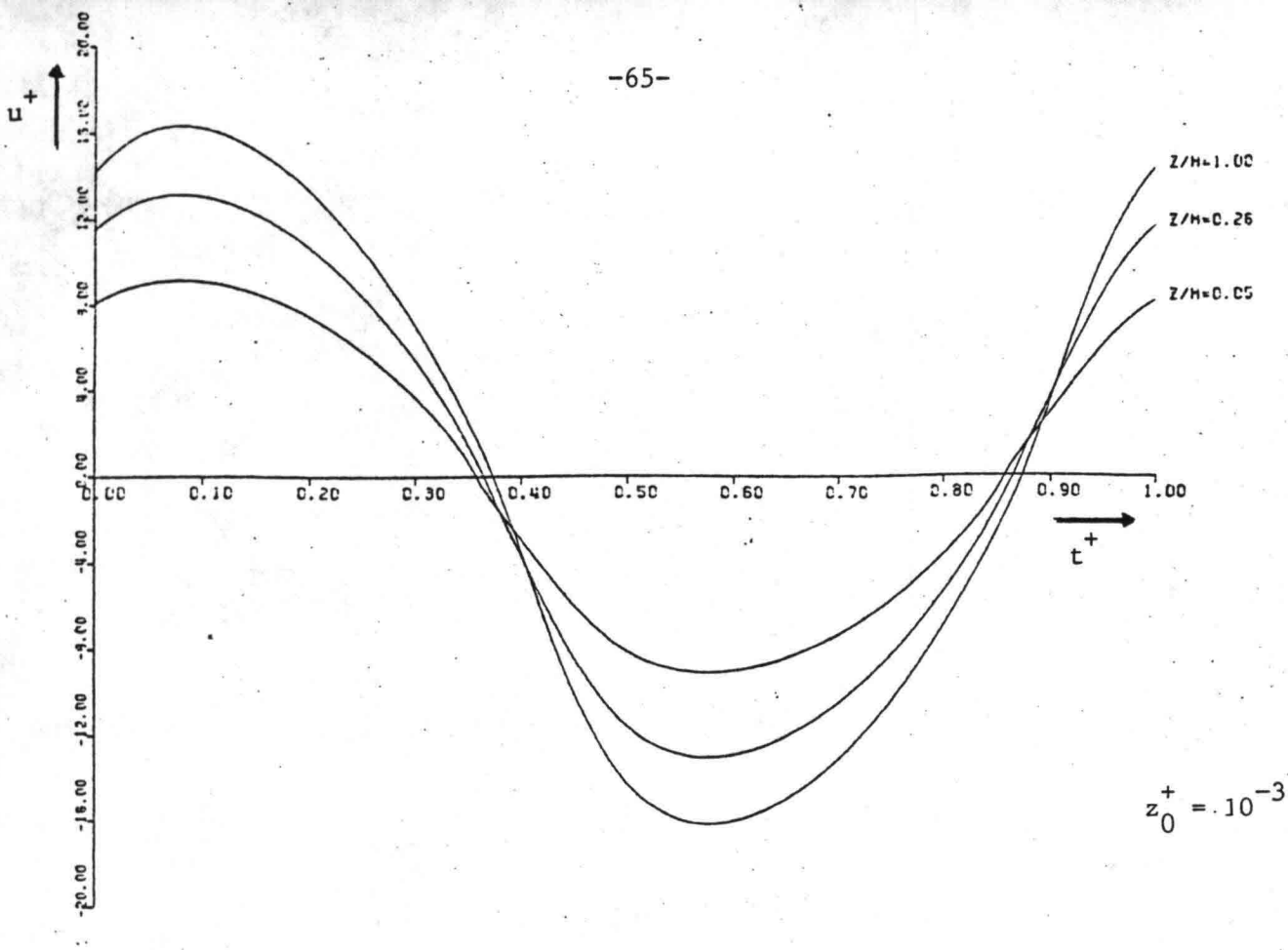

b. Variation of the velocities at various depths over the tidal cycle calculated with the simple eddy viscosity model.

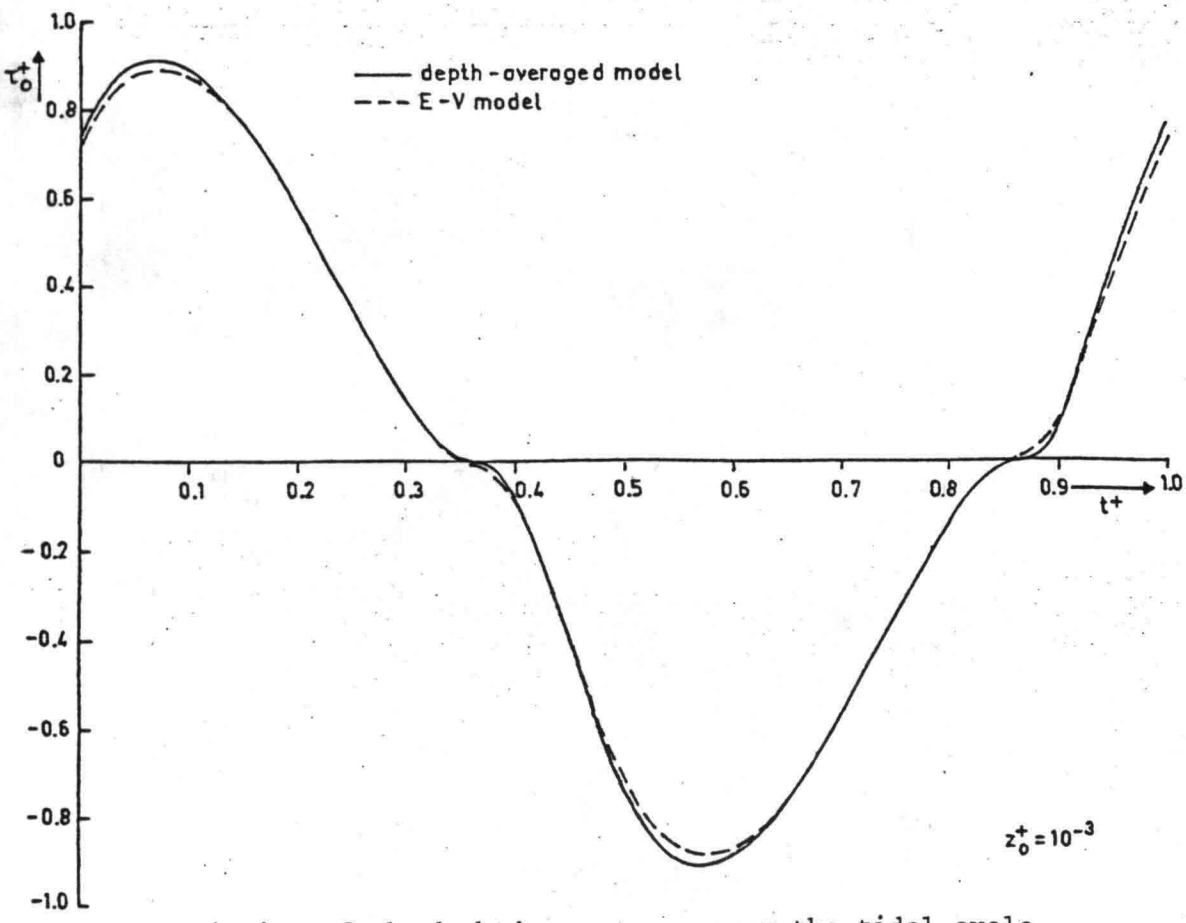

c. Variation of the bed shear stress over the tidal cycle.

fig. 18. Comparison of the simple eddy viscosity model and a depth-averaged model

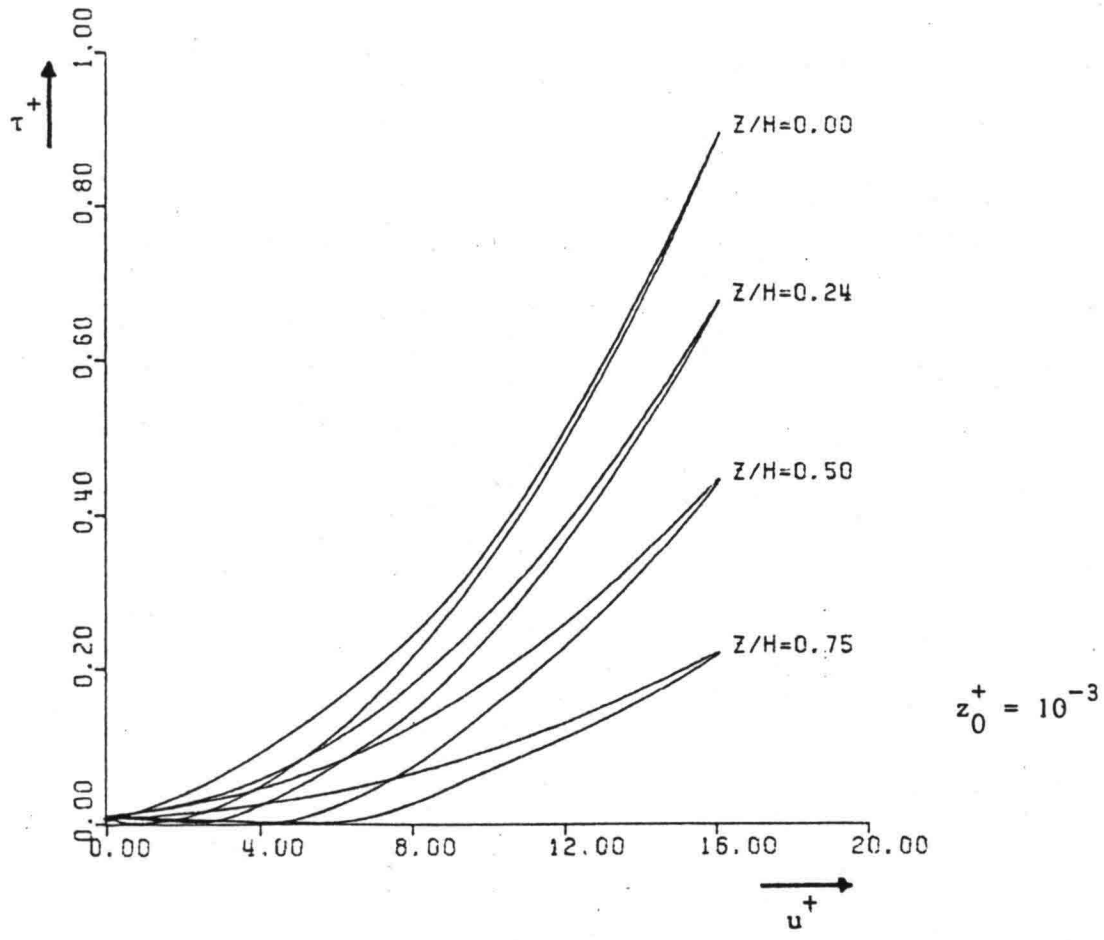

fig. 19. Hysteresis diagram calculated with the k-model.

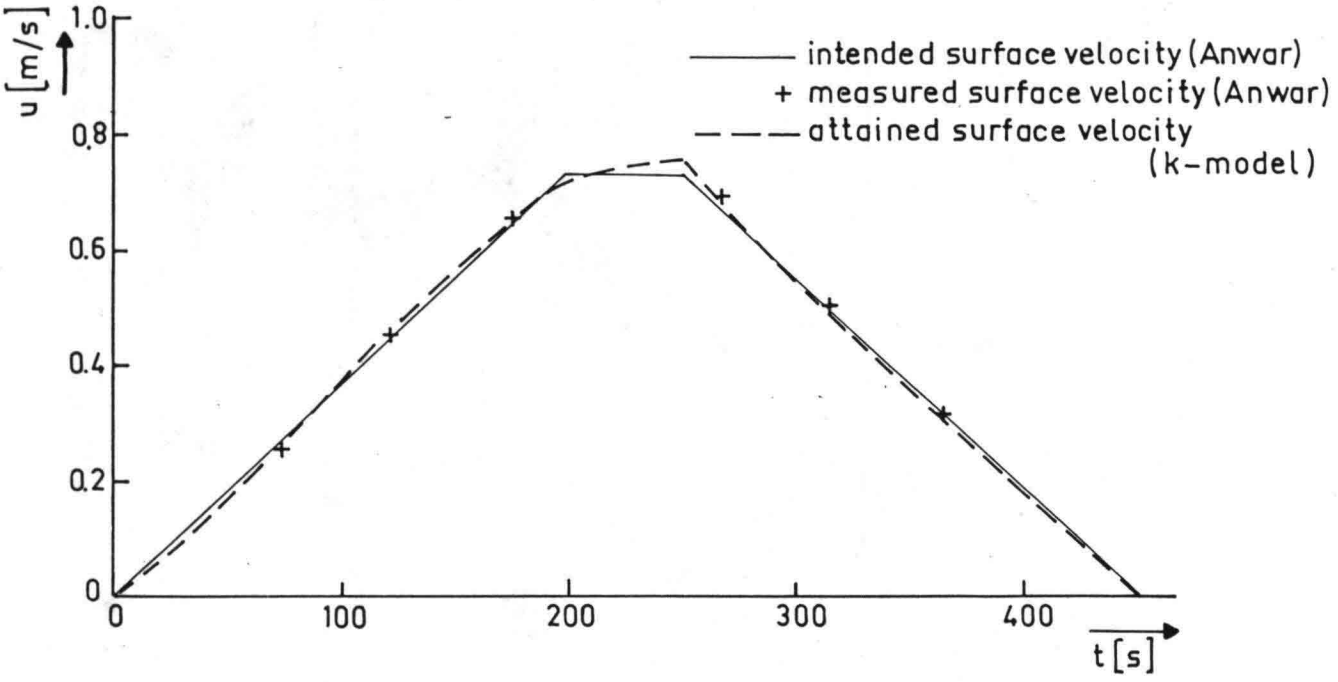

a. Variation of the surface velocity with time.

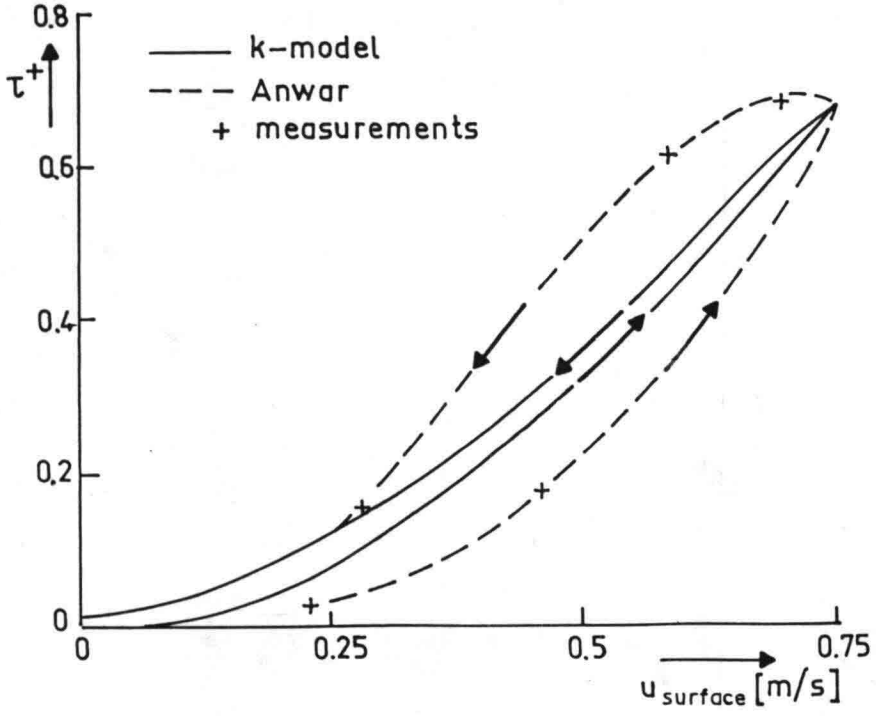

b. Hysteresis diagram ($z^+ = 0.11$)

fig. 20. Comparison of the hysteresis effect calculated with the k-model and the measurements of Anwar and Atkins (1980)

Appendix

Computational Procedure

The transport equations of u, k and ε in the finite difference form are derived by a discretization of the equations over cells around the grid points. u, k and ε are calculated at the grid points. The transports of u, k and ε by diffusion are computed at the cell boundaries, which are situated halfway between the grid points. As an example the expression for the shear stress at A in the k-model is elaborated (see equations 7 and 41)

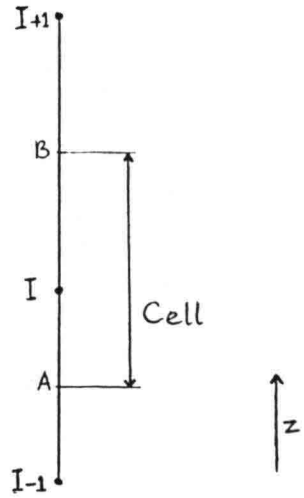

$$\tau(A) = -\nu_t(A)\left(\frac{\partial u}{\partial z}\right)_A \rightarrow -C_\nu \sqrt{\frac{k(I)+k(I-1)}{2}}\, L(A)\, \frac{u(I)-u(I-1)}{z(I)-z(I-1)} \qquad (86)$$

In this expression the value of k at A is replaced by the average of the values of k at the grid points around A.

The rates of production and destruction of u, k and ε within the cells are calculated at the grid points. In most cases this calculation is straightforward. The expressions for the production of k and ε, however, contain velocity gradients. Therefore the rate of production of k (and an analogous part of the expression for the rate of production of ε) is replaced by a mean value of the rates of production of k at the cell boundaries.

$$k_{prod}(I) = \frac{\nu_t(A)\frac{\{u(I)-u(I-1)\}^2}{z(I)-z(I-1)} + \nu_t(B)\frac{\{u(I+1)-u(I)\}^2}{z(I+1)-z(I)}}{z(I+1) - z(I-1)} \qquad (87)$$

Each finite difference counterpart of a transport equation is solved by means of a fully implicit banded matrix procedure (IMSL LEQT1B). The finite difference equation to be solved in this procedure is linearized by treating the production terms, the destruction terms and the diffusion coefficients as known quantities, calculated from the previous step.

The bed boundary value for the velocity is introduced by means of a momentum balance equation for a cell around the first grid point. The cell boundary at C is chosen at the same distance of the first grid point as the boundary at D. For the shear stress at C an expression of the following form is used

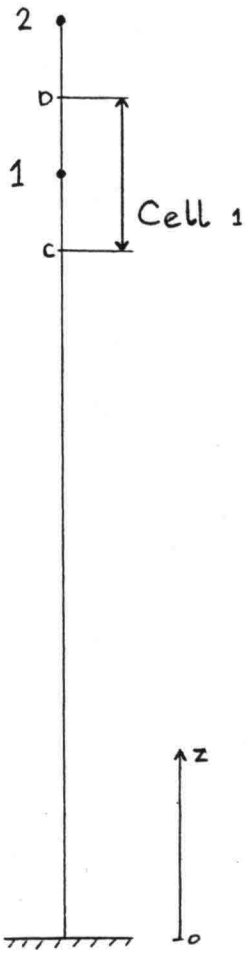

$$\tau(C) = -u_* |u_*| (1-z^+(C)) =$$

$$= - |u(1)| u(1) \frac{\kappa^2 (1-z^+(C))}{\ln^2 (\frac{z(1)}{z_0})} \qquad (88)$$

In this expression for $|u(1)|$ the value calculated at the previous step is used, to linearize the finite difference equation.